SOME INVESTIGATIONS IN TIME DEPENDENT CANONICAL PERTURBATION THEORY

thesis submitted to

The Gujarat University

for

THE DEGREE OF DOCTOR OF PHILOSOPHY

in

PHYSICS

by

MITAXI P MEHTA

December, 1995

PHYSICAL RESEARCH LABORATORY

AHMEDABAD 380 009

INDIA

Certificate

This is to cerify that the thesis entitled SOME INVESTIGATIONS IN TIME DEPENDENT CANONICAL PERTURBATION THEORY contains the original research work of the candidate and that neither this thesis nor any part of it has been submitted for any degree or diploma before.

Mehta MP

(Mitaxi P Mehta)
Candidate

(A R Prasanna)
Guide

Acknowledgments

I am thankful to Dr. B.R.Sitaram for introducing me to the field of classical chaos. His method of analyzing a problem in multidimensional manner has helped me in getting a clear picture of the problem, it has also made me appreciate the generality of mathematical formulation. I have enjoyed working with him over the past five years. I am greatful to Prof. Prasanna for his help. I am thankful to Prof. Parikh and Prof. Khadkikar for taking interest in my work and reviewing it. I wish to thank Prof. Rindani for improving my presentation through his questions and suggestions. I am also thankful to P.R.L. for giving all the facilities for my research work.

Encouragement from Stella and Shwetaketu at the right time has helped me a lot. It is a pleasure to thank Sushma, Anshu, Shikha, Indu, Amruta and Seema for sharing some wonderful times with me. Seema and Indu have been great officemates; discussions with them have been both enjoyable and refreshing. I thank Ramachandran for his help in TEX formating the thesis and Seema and Sushma for proof-reading a part of the thesis. I sincerely thank Mr. Dholakiya and Sai for their efforts to ensure smooth functioning of the computer system and for loading of many useful packages. I thank Vishwanathan for his help on many ocassions.

I thank my parents and parent-in-laws for giving me all the degrees-of-freedom for my studies. Gautam has stood by me through all the troubles. I have enjoyed discussing basic physics and mathematics problems with him. I thank my friends, past and present, research students, PDF's and staff-members of P.R.L., for making my stay at P.R.L. memorable. I thank my sisters Swati, Deepa and Neeta for their love and understanding. I also thank my school teachers Mr. Aniruddha Chhaya and Mr. Rajendra Borisagar for their excellent teaching, unforgettable enthusiasm about scientific ideas and encouragement.

Contents

Chapter 1

Introduction

The investigation of Time Dependent Canonical Perturbation Theory (TCPT) was motivated by the need to understand and analyze Hamiltonian chaos. In this chapter we give an introduction to the field of chaos and some major historical developments in the field. We also give an introduction to Lie method of canonical transformations which has been used in the formalism of TCPT.

1.1 Introduction to Hamiltonian Chaos

Chaos is an interdisciplinary subject results of which are useful in many diverse fields, from Biology and Economy to fluid dynamics and particle physics. It also enters in fundamental subjects like ergodicity and the relation between classical dynamics and quantum mechanics. Study of chaos started in 1885 in the time of Poincare with the famous three body problem [1]. The problem can be stated as follows;

Given three masses interacting only through gravitational interactions, prove either stability or instability of the system.

For this problem one was required to determine whether the three bodies will collapse into each other, go away from each other or will remain in the same state as three separate objects at finite distances from each-other in the asymptotic limit of time. Physical examples of this mathematical problem are, system of earth, moon and sun

or the system of two planets and an asteroid.

The problem turns out to be non-integrable, i.e. it is not possible to solve for the differential equations of the system either in terms of known functions or in terms of quadrature, further for a range of values of masses the system exhibits random dynamics. This kind of random evolution of a dynamical system is known as chaos. Chaos appears when the equations governing the evolution of the system are nonlinear. Though not all the nonlinear systems are chaotic, the problem of chaos appears in most of the non-linear systems encountered in different branches of science.

Dynamical systems can be divided in two classes,
(1) discrete systems, where dynamics is defined by maps, and
(2) continuous systems, where dynamics is defined by a set of differential equations. Continuous systems can be further divided in two subclasses, (1) Hamiltonian systems, (2) Non-Hamiltonian systems. In this thesis we shall be discussing application of the TCPT to Hamiltonian chaos. Following section gives an introduction to the concept of integrability in Hamiltonian systems.

1.1.1 Integrability in Hamiltonian Systems

An n-degree-of-freedom (n-DOF) Hamiltonian system is described by following $2n$ equations,

$$\begin{aligned} \frac{dq_i}{dt} &= \frac{\partial H}{\partial p_i} \\ \frac{dp_i}{dt} &= -\frac{\partial H}{\partial q_i} \end{aligned} \tag{1.1}$$

where $i = 1, 2, \ldots, n$ (if not mentioned explicitly, the subscripts i, j, k are to be understood as dummy variables taking the values from 1 to n). H is the Hamiltonian, which is a function of the phase-space variables q_i and p_i. The variables q_i and p_i are said to be conjugate to each other.

Liouville proved the following for Hamiltonian systems (see [2] and [3]);
For an n-DOF Hamiltonian system, where H is analytic in a given domain $\mathcal{D}$ of phase-space and if n uniform integrals $I_1, \ldots, I_n$ in involution are known in a domain $\mathcal{D}'$ of phase-space belonging to $\mathcal{D}$ then in $\mathcal{D}'$ the system is integrable, i.e. reducible to quadratures.
In other words if the following conditions are satisfied then the system is integrable,

$$\begin{aligned} \{I_i, H\} &= 0 \qquad && \text{constancy} \\ \{I_i, I_j\} &= 0 \qquad && \text{mutually involutive} \end{aligned}$$

where the bracket $\{\,,\,\}$ represents the Poisson bracket. Given these constants of motion one can construct a canonical transformation from the coordinates (q_i, p_i) to the action-angle variables (I_i, θ_i), where I_i are the action variables and θ_i are the conjugate angle variables. In this coordinate system the equations of motion (EOM) can be trivially solved. For non-integrable Hamiltonian systems it is not possible to find such constants of motion.

If the Hamiltonian system is integrable, the Hamiltonian in the transformed coordinates is a function only of the action variables, i.e., $H(q_i, p_i) = H(I_i)$. The equations of motion are,

$$\begin{aligned} \frac{dI_i}{dt} &= 0 \\ \frac{d\theta_i}{dt} &= \frac{dH}{dI_i} = \omega_i \end{aligned}$$

where ω_i are the frequencies which are functions of the action variables I_i. This set of equations can be trivially integrated. Thus existence of action-angle variables shows that the system is integrable.

There is an important theorem for integrable systems which can be stated as follows (see [4] and [2]);
Let the n-DOF Hamiltonian system described by equation 1.1 have n first uniform integrals $I_1, I_2, \ldots, I_n$ in involution. If the equations $I_i = C_i$ define a compact manifold $M = M_c$, at every point of which the vectors ∇I_i are linearly independent in the phase-space of dimension $2n$, then M is a torus of dimension n and the solutions of equations of motion has a quasiperiodic motion on M.

This theorem is important because it ensures that the motion of an integrable system lies on a small n-dimensional region, namely n-torus in phase-space and it does not cover the whole energy surface, which is $2n-1$ dimensional. When an integrable system is perturbed in such a way that the perturbed system becomes chaotic the unperturbed tori are said to be broken. This phenomenon will be discussed in detail in the section on KAM theorem.

1.1.2 Detection of Hamiltonian Chaos

Given a Hamiltonian system there does not exist any general analytical method to decide if it is chaotic. Work done by Ziglin [5], Yoshida [6] and others prove non-integrability only for specific classes of Hamiltonian systems. There exists more general analytical methods to detect chaos like Painleve analysis [7], which predict integrability of a set of differential equations from the behavior of the solutions in the series form of the variable $(t-t_*)$, where t is the independent variable and t_* is the position of the movable singularity of the solution. A system which is integrable according to Painleve's criterion is said to be possessing the Painleve property. Though Painleve's method has been very successful in study of Hamiltonian chaos, so far it is only a conjecture. Further it is possible to make a nonanalytic coordinate change for a system with Painleve property so that the resulting system does not have Painleve property. Because of unavailability of any faithful and simple analytical method to detect chaos one has to resort to numerical methods. There are two main methods to detect chaos numerically, (1) Lyapunov exponents, (2) Poincare sections.

Lyapunov exponents [8] measure the rate of exponential divergence for two nearby orbits. Non-zero Lyapunov exponents for a compact Hamiltonian system in general imply chaos. This method is easy to implement and widely used but it also has some drawbacks. In Hamiltonian systems there can be integrable bounded orbits with non-zero Lyapunov exponents, thus there is a risk (though quite small) of predicting chaos when the system is integrable. We shall be using the method of Poincare sections [9] to detect chaos. Advantages with this method are that it is easy to implement, gives a pictorial view of the system's dynamics and so gives

insight into the phenomenon of breaking of the KAM tori. We give the basic ideas of the method in the following.

For a two-DOF Hamiltonian system the phase-space is four dimensional. For a fixed energy the four independent variables are related by the Energy equation $E = H(q_1, q_2, p_1, p_2)$. To get the Poincare section, the value of one of the variables is fixed to a constant. For example $q_1 = c$, with this condition the system has only two independent variables effectively because condition on q_1 reduces one variable leaving three independent variables and energy equation determines one variable in terms of the remaining two variables. These two independent variables define the Poincare plane. If an orbit is regular, it lies on a torus and thus it's intersection with Poincare plane can be either finite number of points or a regular closed curve. Instead if the orbit is chaotic, it's intersection points on the Poincare plane do not form any regular curve. For a chaotic orbit, the intersection points on the Poincare plane are distributed randomly. Further, intersection of the Poincare plane with a torus is a union of two disjoint sets in general, to select one of the subsets a condition is put on one of the variables of Poincare plane. Appropriate condition in our example can be $p_2 > 0$ or $p_2 < 0$ at the time of intersection.

The problem with the Poincare section method is that there is no unique way to define a proper Poincare plane for a given system, for wrong choices of fixed variable an orbit may never intersect the plane, secondly, this method is useful only when the given system is with 2-DOF, for systems with higher degrees of freedom there is no simple method to view chaos pictorially. With this background in chaos now we can review some major historical developments towards analyzing and understanding chaos.

1.2 Historical Developments

Poincare was the first person to study chaos extensively [1]. Many new techniques have been developed in the field of chaos since the times of Poincare. We shall be concerned here only with the major developments in the canonical perturbation theory and related fields. Poincare in his work developed perturbation theories based

on Hamilton-Jacobi (H-J) formalism of canonical transformation. The H-J theory in itself also gives useful insights into the theory of Hamiltonian chaos as we shall see when we discuss the relation of TCPT to H-J theory. Following section overviews some fundamental aspects of H-J theory.

1.2.1 Hamilton-Jacobi theory

The H-J theory makes use of the fact that evolution of the phase-space variables under the Hamilton's EOM is a canonical transformation. One attempts to construct a time dependent canonical transformation which transforms the phase-space variables at time t to that at $t = 0$. The H-J equation is,

$$\frac{\partial S}{\partial t} + H(\frac{\partial S}{\partial q}, q) = 0$$

where S is the generating function of the transformation which is also called the Hamilton's principle function, it is a function of old coordinates and transformed momenta i.e., $S = S(q, \alpha)$. S generates a transformation from (q, p) to (β, α) so that resulting coordinates and momenta, (β, α) are constant. (β, α) are some functions of coordinates and momenta at $t = 0$. Calculating S is equivalent to solving for the EOM for H. If we assume S to be linear in time, i.e., $S = W - Et$, the H-J equation becomes,

$$H(\frac{\partial W}{\partial q}, q) = E$$

It is this version of H-J theory which was used by Poincare in his work. The function W is called Hamilton's characteristic function.

There is no general method for solving the H-J equation. One special solution of the H-J equation (Hamilton's principle function) is,

$$S = \int L\, dt + constant$$

where L is the Lagrangian of the system. Practically this method is not of much use because to integrate L with respect to time, one is required to know the coordinates and velocities as functions of time i.e. one is required to know the solutions of EOM

beforehand. Another situation where H-J equation can be solved for is the case where separation of the variables is possible, in this case S can be written as

$$S = \sum_i S_i(q_i, \alpha_1, \ldots, \alpha_{i-1}, \frac{\partial S_i}{\partial q_i}, \alpha_{i+1}, \ldots, \alpha_n)$$

where q_i are old coordinates and α_i are transformed momenta. In this case the H-J equation becomes equivalent to a set of n first order, decoupled, ordinary differential equations which are solvable by quadratures.

Though it is not easy to find S for any general problem because existing systematic ways of calculating the generator requires either the system to be separable or the knowledge of solutions beforehand, still the existence of S provides us with useful information. Poincare remarks in his "*New methods of celestial mechanics*" that from the H-J theory it is clear that it is possible to construct a convergent canonical transformation for a chaotic system. This special kind of time-dependent canonical transformation, where transformation equations are the same as solutions to the equations of motion are intimately related to the TCPT transformations considered in this thesis, we shall discuss this relationship in detail in the next chapter

1.2.2 Poincare's Work

Poincare made invaluable contributions in the field of nonlinear dynamics. We shall discuss only one of them here, that is generalization of Lindstedt's method in terms of Hamiltonian dynamics. Before Poincare's work there existed series solution methods of different types for solving nonlinear differential equations. An important series solution method was that of Lindstedt's method ([10],[1]). Lindstedt developed a technique to solve for a set of differential equations of the type,

$$\frac{d^2x}{dt^2} + \eta_1^2 x = \epsilon\phi(x, y, t)$$
$$\frac{d^2y}{dt^2} + \eta_2^2 y = \epsilon\psi(x, y, t)$$

to get a formal series solution in terms of the perturbation parameter. These series solutions had the problem of secular terms where the independent variable appeared algebraically and further, convergence properties of the series were not known.

Poincare formulated the problem in terms of Hamiltonian dynamics. He wrote the solvable part of the differential equation as unperturbed Hamiltonian equations and the full system as perturbation on the unperturbed Hamiltonian. He assumed the perturbed Hamiltonian as well as the action-angle variables for it to be analytic functions of the perturbation parameter ϵ, i.e.,

$$\begin{aligned} H &= H_0 + \epsilon H_1 + \epsilon^2 H_2 + \dots \\ \theta_i &= \theta_i^{(0)} + \epsilon\theta_i^{(1)} + \epsilon^2\theta_i^{(2)} + \dots \\ I_i &= I_i^{(0)} + \epsilon I_i^{(1)} + \epsilon^2 I_i^{(2)} + \dots \end{aligned}$$

He also assumed series expansions in ϵ for the energy and the generating function,

$$\begin{aligned} E &= E_0 + \epsilon E_1 + \epsilon^2 E_2 + \dots \\ W &= W_0 + \epsilon W_1 + \epsilon^2 W_2 + \dots \end{aligned}$$

where $W = W(\theta, J)$ is a function of the old angle variables θ and transformed action variables J. Now, because the canonical transformation given by the H-J theory is given by the relations,

$$\begin{aligned} I_i &= \frac{\partial W}{\partial \theta_i} \\ \phi_i &= \frac{\partial W}{\partial J_i} \end{aligned}$$

where I_i are old action variables and ϕ_i are transformed angle variables, using above relations the H-J equation reduces to,

$$H(\frac{\partial W}{\partial \theta_1}, \dots, \frac{\partial W}{\partial \theta_n}, \theta_1, \dots, \theta_n) = E_0 + \epsilon E_1 + \epsilon^2 E_2 + \dots$$

from which one can calculate W by solving equations at different orders of ϵ. It was found that this method fails due to singularities encountered during calculation of W (the small denominator problem).

Poincare established legitimacy of Lindstedt's method by putting it in Hamiltonian formalism and also generalized it. He showed that Lindstedt's method is divergent in general because of the small denominator problem. We discuss this problem in next section.

1.2.3 The Small Denominator Problem

Given a chaotic Hamiltonian system, it is not possible to get exact solutions for equations of motion or constants of motion using known methods. If the non-integrable Hamiltonian H can be written as a small perturbation on an integrable Hamiltonian H_0, i.e.,

$$H(I_i, \theta_i) = H_0(I_i) + \epsilon H_1(I_i, \theta_i) \tag{1.2}$$

then one can try to solve the problem perturbatively. We wish to construct a canonical transformation such that in the new coordinates I_i', θ_i' the Hamiltonian H becomes integrable, i.e.

$$H(I_i, \theta_i) = H'(I_i') \tag{1.3}$$

The canonical transformation is generated by the function $W(\theta_i, I_i')$, which gives,

$$I_i = \frac{\partial W}{\partial \theta_i} \quad \theta_i' = \frac{\partial W}{\partial I_i'} \tag{1.4}$$

where I_i, θ_i are action-angle variables for H_0 and I_i', θ_i' are action-angle variables for H. One assumes an expansion of W as a series in perturbation parameter [3], $W(\theta, I') = \theta I' + \epsilon W_1(\theta, I') + \ldots$, where the coordinates without subscript means the vector coordinates, for example $I = (I_1, I_2, \ldots, I_n)$. Inserting this series expansion of W in the equation 1.4 and using the new expression for I_i in equation 1.3 yields upto first order in ϵ,

$$\bigtriangledown_{I'} H_0(I') . \bigtriangledown_{\theta} W_1 + H_1(I', \theta) = 0 \tag{1.5}$$

Above equation can be written in terms of Poisson bracket as follows,

$$\{S_1, H_0\} = -H_1 \tag{1.6}$$

Using fourier expansions for W_1 and H_1,

$$W_1 = \sum_{i=0}^{n} W_{1n} e^{i(n \cdot \theta)} \tag{1.7}$$

$$H_1 = \sum_{i=0}^{n} H_{1n} e^{i(n \cdot \theta)} \tag{1.8}$$

in equation 1.5, it can be shown that,

$$W_{1m} = \frac{i H_{1m}(I')}{m \cdot \omega_0(I')} \tag{1.9}$$

where m is a number vector, components of which are integers and ω_0 are unperturbed frequencies i.e. $\omega_0 = \frac{\partial H_0}{\partial I}$. It is the denominator in equation 1.9 which makes the calculation of canonical transformation impossible in certain regions of phase-space. The meaning of the denominator being zero is that the unperturbed motion has a closed orbit. Thus in the regions of phase-space where unperturbed frequencies are commensurate, the corresponding Fourier component of the generator becomes infinity and so Fourier sum for W_1 becomes divergent [3]. Even in the case where the frequencies are not commensurate it is always possible to find some m for which the denominator becomes very small, again leading to divergence. Thus it is not possible to use the canonical perturbation theory to solve for a non-integrable Hamiltonian system because of the small denominator problem.

A break-through came in the field with the KAM theorem. In the next subsection we will have a brief overview of the KAM theorem.

1.2.4 The KAM theorem

The KAM theorem is the major advancement in the field of chaos after the work of Poincare. It was first outlined by Kolmogorov in 1954, afterwards it was proved by Moser (1962), and Arnold (1963) for maps and Hamiltonian systems respectively (see Gia Caglia [2], Arnold [11] and Wiggins [12] for details). The statement of the theorem is;

If the unperturbed vector field is given by,

$$\begin{aligned} \frac{dI}{dt} &= 0 \\ \frac{d\theta}{dt} &= \nabla_I H_0(I) \end{aligned}$$

and if the following condition is satisfied,

$$det[\nabla_I^2 H(I)] \neq 0$$

then "most" of the invariant tori persist for sufficiently small ϵ. The motion on these surviving tori is quasiperiodic, having $m \leq n$ rationally incommensurate frequencies. The invariant tori are dense in the sense that the Lebesgue measure of the complement of the union of the preserved tori is small when ϵ is small.

The theme of KAM is to select a torus on which frequencies are sufficiently irrational and apply perturbation theory on it. The irrationality condition ensures nonsingular generator of canonical transformation. The Hamiltonian found after canonical transformation is taken as the unperturbed Hamiltonian for the next step and the same procedure is repeated. The change in unperturbed Hamiltonian at each stage makes the convergence of the perturbation theory faster compared to the usual perturbation theory where the initial Hamiltonian remains unchanged, thus KAM is called a superconvergent perturbation theory. KAM is function space analog of the Newton-Raphson method.

Let us discuss the conditions for KAM theory to be convergent in detail;
(1) The unperturbed torus on which the calculations are applied should be sufficiently irrational. Kolmogorov proved that if the unperturbed frequencies are sufficiently irrational then the approximation method for accelerated convergence can be applied without encountering the problem of small denominators. He also proved that if the frequencies are sufficiently irrational at the first step of calculation then the total iterated canonical transformation gives convergent results.

(2) The unperturbed motion is non-degenerate, i.e., $det[\nabla_I^2 H(I)] \neq 0$ which can be also written as,

$$det \frac{\partial \omega_{0i}}{\partial I_{0j}} \neq 0 \tag{1.10}$$

where ω_{0i} are unperturbed frequency components and I_{0j} are unperturbed action variables. This condition can be interpreted as all the unperturbed frequencies are functionally independent. This condition ensures that the unperturbed frequencies are in general linearly independent and so irrational. In other words, the resonant unperturbed tori are of Lebesgue measure zero (but at the same time dense on energy surface). Now one condition for KAM method to give convergent results is that the unperturbed frequencies should be sufficiently irrational, thus condition of non-degeneracy implies that most of the unperturbed tori are preserved under small perturbations.

We shall illustrate some number theoretic ideas of KAM for the two degrees of freedom case in the following. Given a ratio $\sigma = \frac{\omega_{01}}{\omega_{02}}$ (where ω_{01} and ω_{02} are unperturbed frequencies), it is possible to approximate it using continued fraction representation

[3]. At the n^{th} stage of approximation one gets,

$$| \sigma - \frac{r_n}{s_n} | < \frac{1}{s_n s_{n-1}}$$

where $\frac{r_n}{s_n}$ is the approximation for σ at the n^{th} stage, with $s_n \geq s_{n-1}$. Now the condition for destruction of tori is as follows,

$$| \sigma - \frac{r}{s} | < \frac{K(\epsilon)}{s^{2.5}}$$

where $K(\epsilon)$ is independent of r and s and goes to zero as $\epsilon \rightarrow 0$. This condition is stricter than that found from continued fraction representation and so not all the frequency ratios will satisfy the condition for tori destruction. Thus there is a non-zero measure of preserved tori.

KAM does not give a global perturbation theory, rather it provides perturbation theory on a single sufficiently irrational tori. KAM holds in those regions of phase space where the small denominator problem does not exist. Thus it does not provide any insight into the small denominator problem or in the mechanism of tori breaking. Further, because KAM has been formulated for quite general Hamiltonian systems, it's results turn out to be too strict for many practical situations. KAM predicts break-down of rational tori for extremely small value of perturbation parameter, whereas for most of the Hamiltonian systems studied so far the numerical evidence shows the motion to be regular for much higher values of ϵ.

One important technique that makes the scope of application of KAM much wider is that of the renormalization [13]. Using renormalisation method one can apply KAM theory to analyze stability of a preserved torus for much higher value of the perturbation parameters than in general allowed by KAM. In renormalization method the question of stability of a given torus $\mathcal{T}_0$ for a Hamiltonian system H, for which the perturbation parameter is outside the region of convergence given by KAM is addressed.

Suppose that the given preserved torus $\mathcal{T}_0$ is enclosed between two higher order resonances, R_1 and R_2. One truncates the Hamiltonian H neglecting terms other than R_1 and R_2 in the perturbation part. A renormalisation transformation Γ_r, which is a combination of coordinate transformation and reparametrization of the

perturbation parameters is applied on this truncated Hamiltonian system. The transformation is selected in such a way that the resulting Hamiltonian is similar to the one with which one started. The transformed torus $\mathcal{T}_0'$ is still preserved and is enclosed between two higher order resonances which may be of different order than before. The transformed Hamiltonian will in general have other resonances away from $\mathcal{T}_0'$, which are to be neglected and the same procedure is repeated. If under these iterations of the transformation Γ_r, the amplitude of the two resonances decreases, the resulting system becomes a system with small perturbation parameter, thus KAM theorem can be applied to it. Thus with renormalization method one can reduce the ϵ value so that the torus comes into convergence region of KAM. If instead of decreasing, the amplitude of the resonances increases then it can be said that with increase in perturbation the torus under consideration will break-down.

Though the KAM theorem does not get rid of the small denominator problem, it gives a superconvergent perturbation theory, proves its convergence away from the region of small denominators and gives a criteria as to where the theory will give convergent results. Because of the condition of non-degeneracy KAM can not be applied to those Hamiltonian systems where the unperturbed Hamiltonian is harmonic-oscillator (and also to any other system which has degenerate unperturbed frequencies), for these systems Gustavson developed a method based on Birkhoff normal form theory, we shall discuss this technique in next subsection.

1.2.5 Gustavson's Normal Forms

Gustavson used Birkhoff's normal form method ([14],[15]) to approximate a chaotic Hamiltonian system by an integrable one in the neighborhood of a fixed point. This method relies on successive canonical transformations of the phase-space coordinates so that the resultant Hamiltonian is integrable if truncated. The outline of the method is as follows.

Let us assume that a Hamiltonian $H(q,p)$ is given which is a power series in the phase-space variables (where q and p are n-vectors). Let us further assume that H is convergent in the neighborhood of the fixed point $q = p = 0$. H can be written

as sum of homogeneous polynomials,

$$H(q,p) = H^{(2)}(q,p) + H^{(3)}(q,p) + \dots \tag{1.11}$$

where the superscripts denote the degree of homogeneity and $H^{(2)}$ is the harmonic oscillator Hamiltonian,

$$H^{(2)}(q,p) = \sum_{\nu=1}^{n} \frac{\alpha_\nu}{2}(q_\nu^2 + p_\nu^2)$$

Let us define the operator,

$$D = \sum \alpha_i (p_i \frac{\partial}{\partial q_i} - q_i \frac{\partial}{\partial p_i})$$

An expression G(q,p) is said to be in normal form if $DG = 0$. Note that the operator D is the same as the time derivative operator for the Harmonic oscillator Hamiltonian, thus the condition for an expression to be in normal form is the same as the condition for constant of motion under $H^{(2)}$. We shall denote a homogeneous polynomial of degree n, which is in normal form by $\Gamma^{(n)}$. Our aim is to construct a canonical transformation so that the given Hamiltonian in the new coordinates is in normal form, for that purpose let us assume that the Hamiltonian in 1.11 is in normal form upto degree $s-1$ and it is written in terms of the transformed variables (q,p) which are composite of the earlier $s-3$ canonical transformations (the Hamiltonian was in normal form upto degree 2 initially).

We want to construct a canonical transformation from (q,p) to (ξ,η),

$$q = \xi + \phi(\xi,\eta)$$
$$p = \eta + \psi(\xi,\eta)$$

such that the resulting Hamiltonian system is in normal form upto degree s of homogeneity. Suppose the transformation is generated by a function $W = q \cdot \eta + W^s(q,\eta)$, which gives the transformation equations,

$$p = \frac{\partial W}{\partial q} = \eta + \frac{\partial W^s}{\partial q}$$
$$\xi = \frac{\partial W}{\partial \eta} = q + \frac{\partial W^s}{\partial \eta}$$

where W^s is a homogeneous polynomial of degree s. The transformation that we are looking for is such that,

$$H(q, \eta + \frac{\partial W^s}{\partial q}) = \Gamma(q + \frac{\partial W^s}{\partial \eta}, \eta)$$

where $\Gamma(\xi, \eta) = \sum_{r=2}^{\infty} \Gamma^r(\xi, \eta)$ and upto $r = s - 1$, $\Gamma^r = H^r$. This gives an equation determining W^s,

$$DW^s(x, \eta) = -H^s(x, \eta) + \Gamma^s(x, \eta)$$

where in definition of D, p is replaced by η.

Now the domain of the operator D can be written as union of two subspaces $D = \mathcal{N} \bigcup \mathcal{R}$ where $\mathcal{N}$ and $\mathcal{R}$ are null and range spaces of D respectively, so that if $P^s \in \mathcal{N}$ then $DP^s = 0$. It is possible to write H^s uniquely as $H^s = R^s + N^s$ where R^s and N^s are members of $\mathcal{R}$ and $\mathcal{N}$ respectively. By choosing $DW^s = R^s$ one gets $\Gamma^s = N^s$ thus the new Hamiltonian is in normal form upto degree s.

Gustavson's method is very useful in studying the dynamics of a chaotic system in regular regime. This technique was applied to the Henon-Heiles (H-H) Hamiltonian system by Gustavson [15]. His results were shown on Poincare sections and were compared with the numerical calculations of Poincare sections at corresponding energies. The numerical studies of the Henon-Heiles system shows that the system is integrable upto energy $= \frac{1}{12}$ for $\epsilon = 1$; for $\frac{1}{12} <$ energy $\leq \frac{1}{6}$ the motion is quasi-chaotic, and beyond energy $= \frac{1}{6}$ the motion is non-compact (there are non-compact orbits also below energy $= \frac{1}{6}$ which are not considered). The system shows increase in chaotic behavior with increase in energy. Gustavson's results are in good agreement with the numerical results upto energy $= \frac{1}{12}$, beyond this energy the numerical calculations for Poincare section shows regions in phase-space which are not foliated by regular curves whereas the normal-form calculations show regular motion everywhere on the energy surface. Thus in chaotic regime Gustavson's method does not converge.

In contrast to KAM, Gustavson's method is applicable only when the unperturbed Hamiltonian is harmonic oscillator (unperturbed frequencies are degenerate), thus KAM and Gustavson's method are applicable to two disjoint classes of Hamiltonian

systems. We shall show analytically as well as numerically that the TCPT can be applied to Hamiltonian systems belonging to both these classes.

1.3 The Lie Canonical Transformation

Canonical transformations are those transformations of the phase-space coordinates under which the Hamiltonian equations of motion remain unchanged. One way of defining canonical transformation is as follows ([16],[17]);
Suppose given phase-space coordinates (q,p) are transformed to new coordinates (ξ,η) such that the old and new coordinates are related by $\xi = \xi(q,p)$ and $\eta = \eta(q,p)$. If $f(q,p)$ and $g(q,p)$ are some functions over phase-space which become $f'(\xi,\eta), g'(\xi,\eta)$ under the transformation and if the Poisson bracket remains invariant under the transformation, i.e.

$$\{f,g\}'_{(q,p)} = \{f',g'\}_{(\xi,\eta)}$$

then the transformation is called canonical transformation.

Hamilton's equations of motion in Poisson bracket form are,

$$\frac{dq}{dt} = \{H,q\}$$
$$\frac{dp}{dt} = \{H,p\}$$

because Poisson brackets are preserved in the transformed coordinates, Hamiltonian equations are also preserved, with Hamiltonian written in the new coordinates. For many Hamiltonian systems the EOM become very simple in some specific phase-space coordinates, because of this the study of canonical transformations is important.

The usual way of defining canonical transformations is as follows; if $S(q,P)$ is some well defined function then it generates the following canonical transformation,

$$p = \frac{\partial S}{\partial q}$$
$$Q = \frac{\partial S}{\partial P}$$

and the new Hamiltonian K is,

$$K = H + \frac{\partial S}{\partial t}$$

S is called the generator of canonical transformation. There are different ways of writing S as a function of mixed variables but essentially S is a function of half of the old phase-space coordinates and half of the transformed coordinates. We shall be calling this generating function which is defined in usual method as the Goldstein generator and the transformation generated as the Goldstein transformation for convenience.

In classical way of defining canonical transformation one does not get a relation between old and new coordinates directly, to get such relationship one has to invert the canonical transformation equations. Because of this it is difficult to work with Goldstein transformations. Unlike the usual method of doing perturbation theory, we have worked with Lie method of canonical transformations (LCT) (for detailed formalism of Lie canonical transformations see [17]). The Lie generator F, which is a function of phase-space coordinates, defines a continuous canonical transformation. Unlike the Goldstein generator the Lie generator defines a one parameter group of transformations. The Lie canonical transformations have been well-studied by Deprit and Hori [18] and successfully applied to Plasma physics problems by Kaufman [19].

The advantage with Lie generator is that one does not work with mixed variables as argument of the generating function, the generating function is either a function of old variables or that of the transformed variables. Thus the transformation equations take a simple form and give direct relationship between old and new coordinates. According to our conventions a Lie generating function G is to be considered as the Poisson-bracket operator $\{G, \}$ when exponentiated and a function over phase-space otherwise. Thus $e^{\delta G}$ is the operator,

$$e^{\delta G} = 1 + \delta\{G, \} + \frac{\delta^2}{2!}\frac{\{G, \{G, \}\}}{2!} + \ldots$$

where 1 is the identity operator and δ is a parameter that can take continuous values. For each value of δ, G defines a Lie transformation as shown above (Note that G has to be independent of δ for the transformation formula to be valid). The result

of the operator $e^{\delta G}$ operating on some phase-space function A is another function A' given by,

$$A' = e^{\delta G} A = A + \delta\{G, A\} + \frac{\delta^2}{2!}\frac{pG\{G, A\}}{2!} + \ldots$$

If G is an explicit function of δ then the Poisson bracket has to be redefined as $\{,\} \rightarrow \frac{\partial}{\partial \delta} + \{,\}$ and the same formulae as for the case where G is independent of δ are valid.

If a Hamiltonian H_0 is transformed to H by a Lie transformation, i.e., $e^{\delta G} H_0 = H$ (where H is still written in the old coordinates) then the solutions of EOM for H_0, ξ_i' are mapped into solutions of EOM for H, ξ_i by,

$$\xi_i = e^{-\delta G} \xi_i' \tag{1.12}$$

and if H is written in terms of the old action-angle variables, (I, θ) then constants of motion I_i' for H are related to constants of motion I_i for H_0 by,

$$I_i' = e^{\delta G} I_i \tag{1.13}$$

We shall prove these relationships in the next chapter.

The disadvantages with LCT are as follows;
The transformation generated gives the new coordinates in terms of an infinite series in δ, where the coefficients of δ are functions of old coordinates. Similarly the transformed Hamiltonian is also written in terms of an infinite series in δ. In specific cases it may be possible to sum up these series to give a finite form but in general one has to work with the infinite series. If δ can be assumed to be small then the series can be truncated to get an approximate transformation. Secondly the Lie method can be used only when the transformation is continuous whereas Goldstein generator can also give discrete canonical transformations.

Before concluding this section we shall illustrate how the small denominator problem translates into the LCT notations. The canonical transformation that one is looking for is the one that transforms H_0 to $H = H_0 + \epsilon H_1$, i.e.,

$$e^{\epsilon F_1} H_0 = H_0 + \epsilon H_1$$

comparing $O(\epsilon)$ terms in both the sides,

$$\{F_1, H_0\} = H_1 \tag{1.14}$$

This equation is the same as equation 1.6 in the small denominator problem but with a sign change and with the difference that S_1 was written in mixed coordinates whereas F_1 is written in the old action-angle coordinates. As in the small denominator problem, writing Fourier expansions for F_1 and H_1 in the above equation yields,

$$F_{1n} = \frac{H_{1n}}{i(n \cdot \omega)} \tag{1.15}$$

which is the small denominator problem. It is easy to see that both F_1 and S_1 give the same result upto $O(\epsilon)$. The Goldstain transformation upto $O(\epsilon)$ generated by $S = S_0 + \epsilon S_1 = I' \cdot \theta + \epsilon S_1(I', \theta)$ is given by,

$$I = \frac{\partial S}{\partial \theta} = I' + \epsilon \frac{\partial S_1}{\partial \theta}$$
$$\theta' = \frac{\partial S}{\partial I'} = \theta + \epsilon \frac{\partial S_1}{\partial I'}$$

which can be written as

$$I' = I - \epsilon \frac{\partial S_1(I, \theta)}{\partial \theta}$$
$$\theta' = \theta + \epsilon \frac{\partial S_1(I, \theta)}{\partial I}$$

considering terms of $O(\epsilon)$. The transformation equations generated by F_1 are,

$$I' = e^{\epsilon F_1} I = I + \epsilon \frac{\partial F_1}{\partial \theta}$$
$$\theta' = e^{\epsilon F_1} \theta = \theta - \epsilon \frac{\partial F_1}{\partial I}$$

thus $F_1 = -S_1$ and both of them generate the same transformation upto $O(\epsilon)$. This exercise shows that LCT gives the same results as the goldstein notations but in a simpler manner without any need of inversion.

1.4 Plan of The Thesis

Plan of the thesis is as follows; Chapter-2 gives motivation for use of TCPT compared to CPT. We explain the reason of singularity in CPT from many different view

points and show in each situation how TCPT helps in removing the singularities. We give the general formalism of TCPT and discuss the relationship between the TCPT generating function and the Hamilton-Jacobi generating function. Analytical properties of the TCPT generating function are discussed in chapter-3. We show that in contrast to CPT generating functions, the TCPT generating functions can be guaranteed to be nonsingular at each order of calculation for finite time. We also discuss two special cases where a definite prediction can be made about the analytical properties of the total TCPT generating function. Analytical continuation of the generating function is possible when the singularities are isolated, we show this for a 1-DOF example.

Chapters 4 and 5 describe application of TCPT to two specific Hamiltonian systems. In chapter-4 we discuss application of TCPT to the Henon-Heiles system. The generating function, invariants and the mapping relationships are calculated upto third order. Numerical prediction of mapping for higher order perturbation theory are given. To understand the convergence properties of the perturbation series we calculate numerically the radius of convergence for a regular and a chaotic orbit. We also apply the perturbation theory to the anti-Henon-Heiles oscillator to see the effect of non-compactness of the potential on convergence of the perturbation series. We also study the dependence of radius of convergence of TCPT on energy for the Henon-Heiles system.

The Henon-Heiles Hamiltonian is a non-KAM type Hamiltonian because the unperturbed frequencies are degenerate. To show that TCPT can be applied to both KAM-type as well as non-KAM type Hamiltonian systems in chapter-5 we apply TCPT to a KAM-type Hamiltonian system. We do similar numerical studies as in Henon-Heiles case. We also show that this Hamiltonian belongs to the class of Hamiltonian systems discussed in chapter-3 for which analytical properties of the total generating function can be predicted. Finally we conclude with a summary of work done and some open questions.

Chapter 2

The Time-dependent Canonical Perturbation Theory

2.1 Why is time dependence necessary ?

In this chapter we discuss the reasons for failure of usual (time-independent) perturbation theory and the advantages of choosing TCPT. We show theoretically as well as with some simple examples how TCPT helps in getting rid of some of the problems in usual perturbation theory [20].

(1) The idea of canonical perturbation theory is to find a generator of canonical transformation $\mathcal{F}$ such that there is a one to one map between the orbits of the unperturbed Hamiltonian H_0 and that of the perturbed Hamiltonian H, i.e. the following diagram should commute.

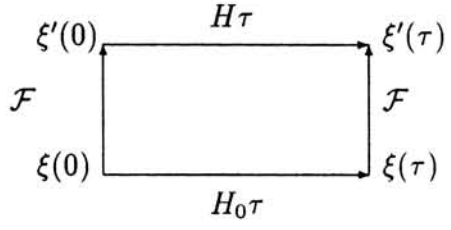

Figure 2.1: **Commutation relation of $\mathcal{F}$ with evolution**

In the figure the symbol $H\tau$ denotes the canonical transformation given by the operator $e^{-H\tau}$ and similarly $H_0\tau$ denotes the corresponding time evolution generator. The symbol ξ denotes phase-space coordinate vector and ξ' denotes the transformed coordinates. The meaning of the diagram is that whether one first evolves a phase-space point $\xi(0)$ in time according to the unperturbed equations to get a new point $\xi(\tau)$ and then apply a canonical transformation $\mathcal{F}$ to get the transformed point $\xi'(\tau)$ or first the canonical transformation $\mathcal{F}$ is applied to $\xi(0)$ to get $\xi'(0)$ and then this point is evolved using the perturbed Hamiltonian EOM, both the way one gets the same end result. The diagram is true for any canonical transformation which transforms H_0 to H but we are interested in the special case where H_0 is an integrable Hamiltonian and H is a chaotic Hamiltonian.

Suppose $\xi(0)$ is a phase-space point on a periodic orbit of H_0 with time period τ, so that the action of the operator $e^{-H_0\tau}$ transforms it back to the same point, i.e., $\xi(0) = \xi(\tau)$. Now if the generator $\mathcal{F}$ is independent of time, i.e., $\mathcal{F}$ depends only on the phase-space coordinates then it will transform both the points $\xi(0)$ and $\xi(\tau)$ to the same point in the transformed coordinates, i.e., $\xi'(0) = \xi'(\tau)$. But this condition implies that if the unperturbed solution ξ is periodic with period τ then the perturbed solution is also periodic with the same time period. In general this can not be true because as we know most of the phase-space of the perturbed Hamiltonian is covered by a single chaotic orbit which never comes back to it's starting point. Thus if a canonical transformation exists which transforms H_0 to H then it has to be either multiple valued function of phase-space so that the same point $\xi(0) = \xi(\tau)$ can be transformed to two different points $\xi'(0)$ and $\xi'(\tau)$, or it has to be time dependent in which case it will give different transformations at $t = 0$ and $t = \tau$ and so the transformed orbit need not be periodic.

(2) Equation 1.14 can be considered as an operator equation in a Hilbert space of periodic functions. Now as we know, an operator equation admits solutions iff the RHS of the equation is orthogonal to the null eigen vector of the adjoint of the operator. In our case the operator in the equation is $A_{op} = \omega \cdot \frac{\partial}{\partial \theta}$, which operates on F_1 to get H_1 in RHS, i.e.,

$$A_{op} F_1 = H_1$$

The operator A_{op} is anti-self-adjoint, so the null eigen vectors of A_{op} and $adj\, A_{op}$

are the same. The eigen vectors of A_{op} are of the form $f(I)e^{i(m\cdot\theta)}$ and the eigen values are of the form $i(m\cdot\omega)$. Thus for equation 1.14 to be solvable, H_1 should be independent of $e^{i(m\cdot\theta)}$ whenever $m\cdot\omega = 0$ or equivalently H_{1m} should be zero whenever $m\cdot\omega = 0$

Above argument shows that by considering equation 1.14 as an operator equation and trying to solve it, the problem encountered is the same as that in the small denominator problem. In the small denominator problem also we required $H_{1m} = 0$ when $m\cdot\omega = 0$ for getting a non-singular solution. One possible reason for the failure is that the assumption with which we started, i.e. F_1 is Fourier expandable in terms of angle variables may be wrong, i.e. F_1 may be an aperiodic function of θ.

(3) Alternatively let us look at this problem as that of solving the equation 1.14,

$$\{F_1, H_0\} = H_1$$

which is a first order partial differential equation. The equation can be solved using method of characteristics (to be discussed in detail later). The formal solution is given by,

$$F_1(z) = \int H_1\, dz \tag{2.1}$$

where z is the characteristic direction of the differential equation. This direction is defined by solutions of unperturbed Hamiltonian equations and it turns out to be the same as the arc parameter t.

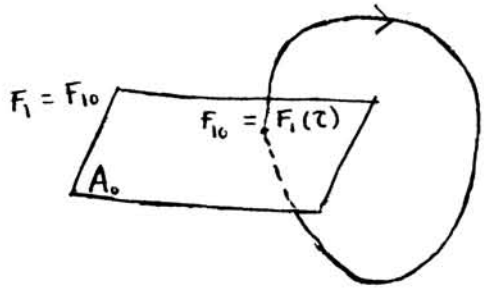

Figure 2.2

To write down the solution explicitly, one requires to give initial value of F_1 at $t = 0$, i.e. F_{10}. Let us consider the situation shown in the figure 2.2 where F_1 is to be calculated for a periodic orbit, the boundary values of F_1 are given on a surface A_0. Now because F_1 is a function of phase-space coordinates when the phase-space point takes it's initial value, F_1 also should take it's starting value. As can be seen

from the formal solution if we insist F_1 to be periodic for a periodic unperturbed orbit, integral of H_1 on that orbit should be zero. But an orbit being closed implies that the corresponding frequencies are commensurate, i.e. there exists a non-zero number vector m such that $m \cdot \omega = 0$. Now considering the corresponding Fourier component H_{1m} and assuming it to be non-zero gives the old small denominator problem, so for the generator to be finite H_{1m} has to necessarily be zero. Analyzing the situation differently, if integral of H_1 over the unperturbed orbit is non-zero then with increase in time $\int H_1 dz$ over the closed orbit keeps increasing and in the limit $t \to 0$, the integral becomes ∞. This explains appearance of singularity in usual canonical perturbation theory when $H_{1m} \neq 0$ and $m \cdot \omega = 0$.

It is easy to see that the condition $H_{1m} = 0$ when $m \cdot \omega = 0$ is not satisfied in general. One example is the case where H_1 is a function only of the action variables. In this case the only non-zero Fourier component of H_1 which is the component with zero number vector m is non-zero i.e. $H_{10} \neq 0$ but the corresponding $m \cdot \omega = 0$. In such cases F_1 turns out to be singular. One can get rid of the problem by making F_1 a multiple valued function of phase-space variables. We show in the following that this property of F_1 being ill-defined can be removed by making it explicitly time-dependent.

(4) Interpreting the above situation in a different manner; let us assume that H_1 contains a piece which is constant over the unperturbed trajectory, i.e.,

$$H_1 = f(I) + g(I, \theta)$$

then from the formal solution,

$$F_1(z) = \int H_1 dz = f(I)z + \int g(I, \theta) dz$$

thus F_1 will contain a piece which is linear in time. If we substitute back the characteristic variable z in terms of the phase-space variables from $\theta = \theta_0 + \omega z$, we get a term which is linear in θ. Now a function which is linear in θ is an aperiodic function of θ and so it can not be Fourier expanded. This result is in agreement with our analysis in (2).

Now as we have seen if $m \cdot \omega = 0$ and $H_{1m} \neq 0$ then one encounters the small denominator problem and it is exactly in such cases that we expect F_1 to be aperiodic

in θ, from this we can say that the small denominator problem comes-up because we are working with Fourier expansion of an aperiodic function. If the phase-space is extended to include time then an unperturbed orbit never closes into itself because all the orbits travel forward in time and the time dependence of the transformation will arise naturally from the part of H_1 which is constant over unperturbed orbit.

(5) A well defined canonical transformation which is not explicitly dependent on time is equivalent to a coordinate transformation of phase-space variables. One can not expect such a transformation to change the dynamical features of the motion like topology of an orbit or that of an energy-surface. It is possible to change topology of an orbit by applying a time-dependent canonical transformation. As an example consider a free particle for which the phase-space diagram is straight lines with momenta p_i being constant. If for a given trajectory the coordinates are transformed as $x_i \rightarrow x_i - p_i t$, then the corresponding straight line in old coordinates will now become a point in the transformed coordinates thus changing the topology of the phase space curve.

It is known that when a perturbation on an integrable Hamiltonian results in a non-integrable Hamiltonian there are drastic changes in the topology of the phase-space (e.g. break-down of resonant tori.). It is easy to see how a time-dependent canonical transformation can account for topology change of phase-curves by considering the extended phase-space. In the extended phase-space a fixed point in the usual phase-space diagram becomes a straight line whereas a straight line goes into another straight line. Thus topologically different phase-curves can have the same topology in extended phase-space.

Conclusion from the above discussion is that if a canonical transformation exists which transforms H_0 to H, it should have one of the following properties
a. Ill-defined by being singular(as in the small denominator problem).
b. Aperiodic in angle variables.
c. Time-dependent canonical transformation.
We have assumed $\mathcal{F}$ to be time dependent.

2.2 The Formalism

In order to use TCPT for chaotic Hamiltonian systems, for simplicity of calculations we have introduced the following notation. We take time t as a new DOF and introduce a new phase-space variable T which is conjugate to t. We redefine the initial and the perturbed Hamiltonian as $H_0 \rightarrow H_0 + T$ and $H \rightarrow H + T$ respectively. The Poisson bracket is now defined on the extended phase-space. Now let us solve equation 1.14 in this formalism using the Fourier expansion method. Writing equation 1.14 as a first order partial differential equation in the extendend phase-space we get,

$$\frac{\partial F_1}{\partial t} + \sum_i \frac{\partial F_1}{\partial \theta_i}\frac{\partial H_0}{\partial I_i} - \frac{\partial F_1}{\partial I_i}\frac{\partial H_0}{\partial \theta_i} = H_1 \tag{2.2}$$

Here H_0 is integrable and so it is a function of action variables only, so $\frac{\partial H_0}{\partial \theta_i} = 0$ and derivative of H_0 with respect to the action variables gives the unperturbed frequencies $\omega_i = \frac{\partial H_0}{\partial I_i}$, thus the above equation reduces to,

$$\frac{\partial F_1}{\partial t} + \sum_i \frac{\partial F_1}{\partial \theta_i}\omega_i = H_1 \tag{2.3}$$

Inserting Fourier expansions of H_1 and F_1 and solving for Fourier components of F_1 we get the following,

$$F_{1n} = e^{-\int_0^t i(n\cdot\omega)d\tau} \int_0^t H_{1n} e^{\int_0^\tau i(n\cdot\omega)d\tau'} d\tau + F_{1n0} \tag{2.4}$$

which upon integration yields,

$$F_{1n} = e^{-i(n\cdot\omega)t} H_{1n} \frac{e^{i(n\cdot\omega)t} - 1}{i(n\cdot\omega)} + F_{1n0} \tag{2.5}$$

and thus using $\theta = \theta_0 + \omega t$, the Fourier sum for F_1 is,

$$F_1 = \sum_n H_{1n} e^{i(n\cdot\theta)} \frac{1 - e^{-i(n\cdot\omega)t}}{i(n\cdot\omega)} + F_{10} \tag{2.6}$$

As can be easily checked, unlike the time independent first order generator, this generator of canonical transformation does not become singular when $(n\cdot\omega) = 0$ but in the limit $(n\cdot\omega) \rightarrow 0$ the generator becomes explicitly dependent on time t.

The other way of solving the equation for F_1 which is sometimes more useful is the method of characteristics for solutions of first order partial differential equations.

If we assume the characteristic direction for the equation to be z then the partial differential equation for F_1 corresponding to equation 1.14 is,

$$\frac{dF_1}{dz} = \frac{\partial F_1}{\partial t}\frac{dF_1}{dz} + \sum_k (\frac{\partial F_1}{\partial \theta_k}\frac{d\theta_k}{dz} + \frac{\partial F_1}{\partial I_k}\frac{dI_k}{dz}) = H_1 \tag{2.7}$$

With the formal solution,

$$F_1(z) = \int H_1 dz \tag{2.8}$$

Comparing the coefficients of partial derivatives of F_1 in equation 2.7 with that in the equation 2.2 gives the characteristic equations,

$$\begin{aligned} \frac{dt}{dz} &= 1 \\ \frac{d\theta_k}{dz} &= \omega_k \\ \frac{dI_k}{dz} &= 0 \end{aligned}$$

which can be easily solved as they are the equations of motion for H_0.

$$\begin{aligned} t(z) &= t(0) + z \\ \theta(z) &= \theta(0) + \omega z \\ I(z) &= I(0) \end{aligned}$$

We shall select $t(0) = 0$ for convenience. Using above expressions of phase-space variables in terms of characteristic direction in H_1 in equation 2.8 yields,

$$F_1(z) = \int_0^z H_1(\theta(0) + \omega\tau, I(0), \tau)d\tau + F_1(0) \tag{2.9}$$

in which $\theta(0), I(0)$ and τ are to be substituted back in terms of θ, I and t. The final expression for F_1 becomes,

$$F_1(t) = \int_0^t H_1(\theta + \omega(\tau - t), I, \tau)d\tau + F_1(0) \tag{2.10}$$

It can be easily seen that $F_1(0)$, which is a function of the phase-space variables I, T, θ and t corresponds to an arbitrary canonical transformation which can be selected at $t = 0$. It is also easy to see from the following diagram that application of F_1 is equivalent to using the unperturbed Hamiltonian to go back in time and using the perturbed Hamiltonian to go forward in time, if $F_1(0)$ is selected to give identity transformation.

Figure 2.3: **Commutation relation of F_1 with time evolution when $F_{10} = 0$**

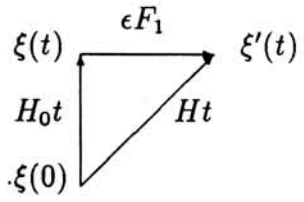

In this thesis we have chosen $F_{10} = 0$ (The commutation relation shown in diagram is correct upto first order in ϵ only).

As we had seen earlier the first order generator F_1 can be calculated using the method of characteristics to be as in equation 2.10. The action of F_1 on H_0 gives rise to higher order terms in ϵ apart from the perturbation part H_1.

$$e^{\epsilon F_1} H_0 = H_0 + \epsilon\{F_1, H_0\} + \frac{\epsilon^2}{2!}\{F_1, \{F_1, H_0\}\} + \dots \tag{2.11}$$

To remove higher order terms form the right side of the equation one uses higher order generators, for example equation for the second order generator is determined by,

$$e^{\epsilon^2 F_2} e^{\epsilon F_1} H_0 = H_0 + \epsilon\{F_1, H_0\} + \frac{\epsilon^2}{2!}\{F_1, \{F_1, H_0\}\} + \dots + \epsilon^2\{F_2, H_0\} + \dots \tag{2.12}$$

Let us select F_2 such that the second order terms in ϵ from the RHS are removed, this gives an equation determining F_2,

$$\{F_2, H_0\} = -\frac{1}{2!}\{F_1, \{F_1, H_0\}\} = -\frac{1}{2!}\{F_1, H_1\} \tag{2.13}$$

Similarly an equation determining F_3 is found by applying a third order canonical transformation $e^{\epsilon F_3}$ and selecting F_3 so that it cancels third order terms in ϵ from the RHS,

$$\{F_3, H_0\} = -\frac{1}{3!}\{F_1, \{F_1, \{F_1, H_0\}\}\} - \{F_2, \{F_1, H_0\}\} \tag{2.14}$$

The transformation upto order n transforms the Hamiltonian H_0 to the Hamiltonian H correctly upto n^{th} order in ϵ. Notice that the equations determining F_1, F_2 and F_3 have the same form,

$$\{F_j, H_0\} = RHS$$

where $j = 1, 2, 3$ and RHS is some function of phase-space variables. Because the equations come in the same form, the procedure can be generalized for an arbitrary order transformation and all the equations can be solved using the same method. In general the partial differential equation determining the $(n+1)^{th}$ order generator can be determined using the following set of equations.

$$H^{(0)} = H_0,$$

$$\{F_1, H_0\} = H_1,$$

$$H^{(n+1)} = e^{\epsilon^{(n+1)} F^{(n+1)}} H^{(n)}, n \geq 0,$$

$$-\{F_{(n+1)}, H_0\} = \text{ coefficient of } \epsilon^{n+1} \text{ in } H^{(n)}, n \geq 1 \tag{2.15}$$

Where the n^{th} order generator is such that it kills terms of order ϵ^n (which are generated by lower order generators) in the following equation.

$$\ldots e^{\epsilon^n F_n} \ldots e^{\epsilon F_1} H_0 = H \tag{2.16}$$

2.2.1 Solutions and Invariants

Using the generators upto order n one can calculate approximate constants of motion which are mutually involutive. These constants are given by,

$$I_i' = e^{\epsilon^n F_n} \ldots e^{\epsilon F_1} I_i \tag{2.17}$$

where I_i represent solutions for equations of action variables of H and I_i' are the constants of motion. The way to calculate I_i' is to calculate the action of the generating functions on I_i symbolically to get an expression in the unperturbed coordinates. In the resulting expression when (I, θ) are evolved according to the EOM of H, the I_i' remain constant.

It is easy to see that I_i' are indeed mutually involutive and are constants of motion from the following,

$$\{I_i', I_j'\} = \{e^{\epsilon^n F_n} \ldots e^{\epsilon F_1} I_i, e^{\epsilon^n F_n} \ldots e^{\epsilon F_1} I_j\} = e^{\epsilon F_1} \ldots e^{\epsilon^n F_n} \{I_i, I_j\} \tag{2.18}$$

but $\{I_i, I_j\} = 0$, hence the I_i' are mutually involutive. I_i' are constants of motion can be shown as follows,

$$\begin{aligned}
\{I_i', H\} &= \{e^{\epsilon^n F_n} \ldots e^{\epsilon F_1} I_i, H\} \\
&= e^{\epsilon F_1} \ldots e^{\epsilon^n F_n} \{I_i, -e^{\epsilon F_1} \ldots e^{-\epsilon^n F_n} H\} \\
&= e^{\epsilon F_1} \ldots e^{\epsilon^n F_n} \{I_i, H_0\} \\
&= 0
\end{aligned} \tag{2.19}$$

where we have used the fact that action variables are constants of motion for unperturbed Hamiltonian, i.e. $\{I_i, H_0\} = 0$.

The mapping from the unperturbed solutions to the perturbed solutions can be derived as follows, suppose ξ_i' represents solutions of EOM of H_0 and ξ_i represent solutions of EOM for H (here $\xi_1 = \theta_1$ etc. for EOM for H and $\xi_1' = \theta_1$ etc. for EOM for H_0), then

$$\xi_i(t) = e^{-tH} \xi_i(0)$$

but from the commutation relation $e^{-\epsilon F_1} e^{-tH_0} = e^{-tH} e^{-\epsilon F_1}$, which holds because F_1 is a canonical transformation we get the following equation,

$$\xi_i(t) = e^{-\epsilon F_1} e^{-tH_0} e^{\epsilon F_1} \xi_i(0)$$

Operating by $e^{\epsilon F_1}$ on both the sides in the above equation yields,

$$e^{\epsilon F_1} \xi_i(t) = e^{-tH_0} e^{\epsilon F_1} \xi_i(0)$$

Now if we define the mapping relation as $\xi_i' = e^{\epsilon F_1} \xi_i$ then,

$$\xi_i'(t) = e^{-tH_0} \xi_i'(0)$$

which is the evolution equation for the unperturbed solutions.

The general mapping equation can be given by,

$$\xi_i = e^{-\epsilon F_1} e^{-\epsilon^2 F_2} \ldots e^{-\epsilon^n F_n} \xi_i' \tag{2.20}$$

where ξ_i' and ξ_i are solutions for unperturbed and perturbed Hamiltonian systems respectively. Equation 2.20 allows one to calculate the solutions for perturbed system accurate upto order n in ϵ once the unperturbed solutions and the generating

function upto order n are known. It should be noted that higher order in ϵ does not mean highly accurate numerical results as time t appears explicitly in the transformation equations, what can be ensured is that for small values of time and away from the singularity in complex ϵ plane above formulae provide very good approximations for the constants of motion as well as the solutions.

2.3 TCPT and the Hamilton-Jacobi theory

One motivation for considering TCPT comes from the Hamilton-Jacobi theory. Poincare believed that the time dependent series solutions of the perturbed system should be convergent because the solution of the Hamilton-Jacobi equation exists [1]. Instead of working in Lie formalism one can as well have time dependent canonical transformation generator which is of Goldstein type, one such generator is the Hamilton's principle function. This generator gives a transformation(in mixed notation) which transforms the phase-space coordinates at time t to phase-space coordinates at time zero and the inverse transformation equations are the solutions of the Hamilton's equations of motion.

The generating function for Hamilton-Jacobi theory, S is given by,

$$\frac{\partial S}{\partial t} + H(\frac{\partial S}{\partial \theta}, \theta) = 0 \tag{2.21}$$

where S is a function of the old angle variables θ_i and the new momenta α_i. If the Hamiltonian H does not explicitly depend on time then one assumes S to be linear in time. Assuming $S = W - Et$, the Hamilton-Jacobi equation becomes,

$$H(\frac{\partial W}{\partial \theta}, \theta) = E \tag{2.22}$$

Instead of taking S to be linearly dependent on time let us assume a general time dependence of S and write power series expansion of S in terms of ϵ,

$$\begin{aligned} H(I,\theta) &= H_0(I) + \epsilon H_1(I,\theta) \\ S(\theta,t) &= S_0(\theta,t) + \epsilon S_1(\theta,t) + \epsilon^2 S_2(\theta,t) + \ldots \\ I &= \frac{\partial S}{\partial \theta} \end{aligned}$$

(We have not shown the constant transformed action variables in the arguments of S). Using these equations in the Hamilton-Jacobi equation 2.21 and equating equal powers of ϵ we get a series of equations determining the S_i. It can be seen that by making S explicitly dependent on time the resulting canonical transformation turns out to be equivalent to transformation given by TCPT.

The relation between the Goldstein type generator S and the Lie generating function F which generates translation in ϵ is given by,

$$\frac{\partial S}{\partial \epsilon} + F(\theta, \frac{\partial S}{\partial \theta}) = 0 \tag{2.23}$$

For the case where S is the solution of Hamiltonian-Jacobi equation this relation is,

$$\frac{\partial S}{\partial t} + H = 0 \tag{2.24}$$

which is the Hamilton-Jacobi equation itself. In H-J equation S generates the canonical transformation which connects the phase-space coordinates at time t to the phase-space coordinates at time $t = 0$, the Hamiltonian generates the same transformation when used as a Lie generating function.

Here it will be worth-while to show a relationship which makes the relationship between the TCPT, the Hamilton-Jacobi theory and the time evolution of the system clear. Suppose that an operator F_{op} defines a canonical transformation (either Lie or Goldstein), then according to the definition of canonical transformations the Poisson bracket should be invariant, i.e.,

$$F_{op}\{H, \phi\} = \{F_{op}H, F_{op}\phi\}$$

where ϕ is some function over phase-space. Now if we write the transformed Hamiltonian as $H' = F_{op}H$ and write adH for the operator $\{H, \}$ then the following two operator relations hold,

$$F_{op}adH = adH'F_{op}$$

which implies,

$$\begin{aligned} F_{op}(t)\sum_{n=0}^{\infty}\frac{t^n}{n!}adH^n &= \sum_{n=0}^{\infty}\frac{t^n}{n!}adH'^n F_{op}(0) \\ \Rightarrow F_{op}(t)e^{-tH} &= e^{-tH'}F_{op}(0) \end{aligned}$$

where the arguments 0 and t of F_{op} indicates that the two operators are to be considered at different times. Now let us select $F_{op}(0)$ to be an identity transformation, then

$$F_{op}(t) = e^{-tH'}e^{tH}$$

thus a canonical transformation which takes EOM of H to that of H' can be written as above mentioned composition of the time evolution of the two Hamiltonian systems, but as we know the H-J generator provides transformation equations which are the same as solutions of EOM, thus the H-J theory,F_{op} and the time evolution of the Hamiltonian systems are closely related and the TCPT generator is effectively the same as F_{op} when at $t = 0$ the TCPT transformation is selected to be identity.

In general one expects the TCPT generator to be singular in ϵ. As is the usual case the unperturbed evolution is always independent of ϵ so all the ϵ singularities of $\mathcal{F}$ should be coming from the time evolution given by the perturbed Hamiltonian system. But the transformation given by $\mathcal{F}$ is composition of the two transformations $\mathcal{F} = e^{H_0 t}e^{Ht}$, thus a non-trivial ϵ singularity structure in $\mathcal{F}$ corresponds to a similar nontrivial singularity structure of S, the H-J generating function.

Chapter 3

Analiticity Properties of the Perturbation Series

In this chapter we discuss analyticity properties of TCPT. This discussion is important in understanding convergence properties of the perturbation series and it also provides insight into results of other methods like KAM and the Gustavson's method. We shall consider two important aspects,

1. The finiteness of each term in the perturbation theory.
2. Analyticity of the total generator $\mathcal{F}$, defined by,

$$\mathcal{F} = \ldots e^{\epsilon^n F_n} \ldots e^{\epsilon F_1} \tag{3.1}$$

3.1 Finiteness of the F_i

For a perturbation series to be convergent there are two requirements, (1) each term in the series should be finite and (2) the series while summed over should give a finite result. Now as we know from the small denominator problem, in the usual way of doing perturbation theory the first order generator turns out to be singular (In fact the same problem persists at all orders). We require the canonical transformation given by different orders of the perturbation theory as well as the total transformation given by composite of transformations at all the orders to be convergent. Thus our first step in the direction of a convergent perturbation theory

is to have the generating functions at different orders to be nonsingular. This result is shown in the following.

It is shown that If F_1 is an entire function of the two variables t and $(n \cdot \omega)$ (and hence of I, if ω's and H_{1n} are entire functions of I), and periodic in θ the same property will hold for generators at all orders [20].
Lemma: *Assume that H_0 and H_1 are analytic in I. Define a sequence of canonical transformations through the equations 2.15:*

$$H^{(0)} = H_0,$$

$$\{F_1, H_0\} = H_1,$$

$$H^{(n+1)} = e^{\epsilon^{(n+1)} F_{n+1}} H^{(n)}, n \geq 0,$$

$$-\{F_{n+1}, H_0\} = \text{ coefficient of } \epsilon^{n+1} \text{ in } H^{(n)}, n \geq 1$$

Then, F_n is an entire function of I and t and is periodic in θ for all $n = 1, 2, \ldots$ (In brief, we shall say that $F^{(n)}$ is regular).

Proof: The proof follows from induction, using the following facts:

(1) If $H^{(n)}$ is regular and $F_{(n)}$ is regular, so is $H^{(n+1)}$: this follows from the fact that the computation of $H^{(n+1)}$ involves the computation of derivatives, which preserves regularity.

(2) The PDE $\{A, H_0\} = G$ has the property that if G is regular, then A is regular; in fact, if $G = \sum G_n e^{i(n \cdot \theta)}$, where the Fourier coefficients are entire functions of I and t, then $A = \sum A_n e^{i(n \cdot \theta)}$, where

$$A_n = e^{-i(n \cdot \omega)t} \int_0^t e^{i(n \cdot \omega)t} G_n dt \tag{3.2}$$

In the RHS $(n \cdot \omega)$ and t appear as arguments of the exponential function which can be singular only when the variable themselves become ∞, further because the integration is to be done for finite real time the integrand remains within the region of analyticity during the integration. Thus the RHS is an integral of an entire function of t and $(n \cdot \omega)$ along a contour which lies within the region of analyticity; hence the conclusion. ∎

Above result shows that the TCPT is successful in removing the problem of singularities in the generating function at each order of calculation, which was encountered in usual perturbation theory. The next question that remains is that of the convergence of the perturbation theory as a whole, i.e., when the total perturbation series is summed will it give convergent result? It should be noted that because now the generating functions are also dependent on time, a higher order calculation in ϵ only does not suffice for high accuracy, value of t also becomes important in determining convergence. We discuss this problem of convergence of the total TCPT series in the next section.

3.2 Convergence of the Perturbation Theory

In calculation of the generating functions at different orders, we have assumed that the total Lie generator $\mathcal{F}$ is analytic in ϵ and $\mathcal{F}$ can be calculated as power series in ϵ from the equation,

$$\mathcal{F} = \ldots e^{\epsilon^n F_n} \ldots e^{\epsilon F_1}$$

If $\mathcal{F}$ has singularities in complex ϵ plane then this power series approximation for $\mathcal{F}$ will converge for that finite radius in ϵ which is defined by the nearest singularity. Thus if $\mathcal{F}$ has a singularity in complex ϵ plane then the mapping and constant of motion approximation will be valid only inside the radius of convergence.

Now the total canonical transformation $\mathcal{F}$ is equivalent to transforming backwards in time using H_0 and then transforming forwards in time using H. Since the first step is independent of ϵ, the analyticity properties of $\mathcal{F}$ is decided by the analyticity properties of the time evolution operator H as a function of ϵ. In general, of course, the analyticity properties of $\mathcal{F}$ as a function of ϵ will depend on t; this is in contrast to the time independent case, where analyticity properties are independent of t. It is not possible to derive general results regarding the analyticity properties of the transformation for any given perturbative Hamiltonian system.

There is no known analytical method to predict complex ϵ singularities. We have developed a numerical method for this purpose. The idea of our method is as

follows. Solutions of the perturbed equations can be calculated from the unperturbed solutions using the equation 2.20. It is also known that the unperturbed solutions are analytic in ϵ (in fact they are independent of ϵ), which implies that any ϵ singularity present in the solutions of the perturbed system has to come from the singularity in $\mathcal{F}$. Thus singularities in perturbed solutions are the singularities of the generating function. To investigate singularities in $\mathcal{F}$ in this manner a Fortran program was developed, we shall discuss this program in the chapter on the Henon-Heiles system.

Once the position of complex-ϵ singularity for a fixed real time is known, it is possible to overcome the convergence problem caused by this singularity, provided the singularity in question is an isolated singularity (which is almost always the case in Hamiltonian quasi-chaos). The way of avoiding convergence problem in perturbation series due to existence of isolated singularity is to analytically continue the generating function, we shall discuss this in detail later.

There are two special cases where definite predictions can be made about analyticity of $\mathcal{F}$.
1. The region in phase space where KAM tori exist.
2. The case where H_0 and H_1 are homogeneous polynomials in the phase space variables.
We discuss these two cases in following two sections.

3.2.1 Relation of $\mathcal{F}$ with $\mathcal{F}_{KAM}$

According to KAM theorem the perturbation theory converges for the irrational tori when the perturbation parameter is small. We show in the following that TCPT will give convergent results in the cases where the KAM generator exists and is analytic in action angle coordinates.

We assume that there exists a time independent canonical transformation $\mathcal{F}_{KAM}$ (calculated using KAM theory) for given irrational frequencies and for a certain value of ϵ. The existence of KAM generator for a torus implies that $\mathcal{F}_{KAM}$ intertwines between the time evolution generated by the unperturbed and the perturbed Hamiltonian systems, which implies that the following diagram commute. This

diagram shows Relation of $\mathcal{F}$ with $\mathcal{F}_{KAM}$.

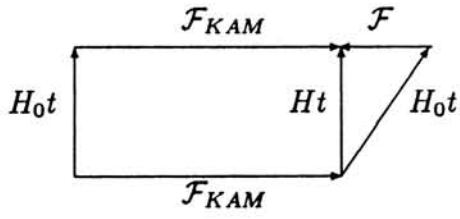

Figure 3.1:**Relation of $\mathcal{F}$ with $\mathcal{F}_{KAM}$**

This means that given a phase-space point (on the KAM torus) one can first apply the canonical transformation generated by $\mathcal{F}_{KAM}$ and then evolve the resultant point under H or one can first evolve the point under H_0 and then apply the canonical transformation generated by $\mathcal{F}_{KAM}$, in both the cases, final result will be the same. We also know that if $\mathcal{F}$ exists, it maps the solutions for H_0 to the solutions of H.

From the diagram one gets the following formula,

$$\mathcal{F} = \mathcal{F}_{KAM}\, e^{-tH_0}\, \mathcal{F}_{KAM}^{-1}\, e^{tH_0} \tag{3.3}$$

thus $\mathcal{F}$ will exist provided the time evolution of $\mathcal{F}_{KAM}$ under the unperturbed Hamiltonian is well defined for real t. In particular, since $\mathcal{F}_{KAM}$ will depend on I, θ and their evolution under H_0 is trivial, $\mathcal{F}$ will be analytic in ϵ provided $\mathcal{F}_{KAM}$ exists. Further, in such a case, $\mathcal{F}$ will be analytic in ϵ for all t, hence existence of $\mathcal{F}_{KAM}$ guarantees convergence of the TCPT.

Above relation provides us with insight into the results of the KAM theorem and the structure of the perturbation theory. KAM theorem guarantees convergence of perturbation theory under the conditions that the unperturbed frequencies are irrational and non-degenerate. Equation 3.3 implies that if KAM theory give convergent results, the usual canonical transformation generator $\mathcal{F}$ will have only isolated singularities in complex-ϵ real time space and so it can be analytically continued.

The KAM theorem does not provide us with any insight in case of rational tori. The method of overlapping resonances give good estimates of the critical energy for chaos to start but does not give any information about nature of the perturbation theory.

We propose that in the case of chaos the singularity structure of $\mathcal{F}$ should be such that it does not allow for analytical continuation in the real-t real-ϵ direction. In the following section we prove a result for a special class of Hamiltonian system which shows that analytical continuation of the generating function may not be possible when the system is chaotic and it's solutions have a natural boundary structure in complex time.

3.2.2 Relation Between Complex-ϵ and Complex-t Singularities

For a class of Hamiltonian systems it is possible to relate the complex-time analytical structure of fully perturbed Hamiltonian systems to the complex-ϵ analytical structure of the canonical transformation which transforms the Hamiltonian with a small ϵ value to the Hamiltonian with a large ϵ value [20].

Let us take a Hamiltonian system where the unperturbed part is homogeneous function of degree m in phase space variables (q_i, p_i) and the perturbation part is homogeneous function of degree n,

$$H(q_i, p_i) = H_0(q_i, p_i) + \epsilon H_1(q_i, p_i); \tag{3.4}$$

For such Hamiltonian systems, it is possible to do a scale transformation of the phase space variables so that the resulting Hamiltonian is the same Hamiltonian, with $\epsilon = 1$ and a constant multiplier. Assuming $n > m$ the transformation is,

$$q_i' = q_i\epsilon^{\alpha}, \;\; p_i' = p_i\epsilon^{\alpha} \tag{3.5}$$

where $\alpha = \frac{1}{n-m}$ and the Hamiltonian becomes

$$H'(q_i', p_i') = \epsilon^{-m\alpha}(H_0(q_i', p_i') + H_1(q_i', p_i')) \tag{3.6}$$

(Note that this transformation is not a canonical transformation, but it transforms the vector field of H at some ϵ to the vector field of H at $\epsilon = 1$.). It is possible to reparametrize the system with ϵ' defined by, $\epsilon = (1 + \epsilon')^{-\frac{1}{m\alpha}}$, this yields,

$$H'(q_i', p_i') = (1 + \epsilon')(H_0(q_i', p_i') + H_1(q_i', p_i')) \tag{3.7}$$

but the above Hamiltonian is equivalent to perturbing the Hamiltonian, $H_{\epsilon=1}(q_i', p_i') = H_0(q_i', p_i') + H_1(q_i', p_i')$ by itself, the perturbation parameter being ϵ', i.e.,

$$H'(q_i', p_i') = H_{\epsilon=1}(q_i', p_i') + \epsilon' H_{\epsilon=1}(q_i', p_i') \tag{3.8}$$

for such a perturbation the first order generator F_1 alone gives the total canonical transformation because $F_1 = H_{\epsilon=1}(q_i', p_i')t$ and all the higher order generators vanish. F_1 can also be treated as the Hamiltonian for ϵ' evolution (except at $\epsilon = 0$ because there the scaling transformation is ill-defined.) because it generates infinitesimal transformation in ϵ'. The ϵ' evolution equations are,

$$\frac{\partial q_i'}{\partial \epsilon'} = \frac{\partial F_1}{\partial p_i'}; \quad \frac{\partial p_i'}{\partial \epsilon'} = -\frac{\partial F_1}{\partial q_i'} \tag{3.9}$$

Now F_1 is the same as $H(q_i, p_i)$ at $\epsilon = 1$, but for an extra multiplier t. So above equations can be rewritten as,

$$\frac{\partial q_i'}{\partial \epsilon' t} = \frac{\partial H_{\epsilon=1}(q_i', p_i')}{\partial p_i}; \quad \frac{\partial p_i'}{\partial \epsilon' t} = -\frac{\partial H_{\epsilon=1}(q_i', p_i')}{\partial q_i} \tag{3.10}$$

But these equations are the time evolution equations for the Hamiltonian $H_{\epsilon=1}$. Thus if $H_{\epsilon=1}$ has singularities in the complex t plane, then a canonical transformation defined by F_1 also will have singularities in the complex $\epsilon' t$ plane, and hence in the complex ϵ plane for a fixed t. Also, the presence of a natural boundary in the complex t plane for the Hamiltonian $H_{\epsilon=1}$ will manifest itself as a natural boundary in the complex ϵ plane for $\mathcal{F}$. For example consider the $t = 1$ case, where the evolution equations for ϵ' are the same as for t and so natural boundaries in complex t plane will manifest itself into that for complex ϵ' plane and hence for complex ϵ plane. Hamiltonian systems with homogeneous perturbation and which have natural boundary structure in complex time plane can be easily found in literature, one such well-studied system is the Henon-Heiles system [21].

In case the singularities of the time evolution operator e^{-tH} in the complex ϵ plane are isolated(which almost always happens in the case of Hamiltonian quasi-chaos), it is possible to use analytic continuation to define F beyond the radius of convergence. However, as the above study shows, the existence of natural boundaries in the complex t plane may imply the existence of similar boundaries in the complex ϵ

plane also. It is possible to study the analyticity properties of F using standard tools for determining the analyticity properties of the solutions of the equations of motion of H. We discuss one such technique in the appendix A-1 in the next chapter.

3.3 Analytical Continuation of the Transformation

A perturbation theory gives convergent results provided the value of the perturbation parameter lies inside the radius of convergence determined by the position of nearest singularity in complex perturbation parameter plane. Thus the TCPT becomes divergent beyond this radius. A way out of this problem is to analytically continue the generator of the transformation.

A two step perturbation theory was worked out. In this theory the range of ϵ for which calculations are to be done is divided in two small steps $\epsilon = \epsilon_1 + \epsilon_2$. The first step of the canonical transformation transforms the initial unperturbed Hamiltonian to the Hamiltonian with perturbation parameter value ϵ_1. In the next step the Hamiltonian resulting from first step is transformed to get the final Hamiltonian with perturbation parameter value $\epsilon_1 + \epsilon_2$.

The transformation equation for a $(2 + 1)$ perturbation theory (second order transformation in first step and first order transformation in second step) is,

$$e^{\epsilon_2 F_{1p}} e^{\epsilon_1 F_2} e^{\epsilon_1 F_1} H_0 = H$$

where F_{1p} is the first order generator for the second step. Which can be calculated as following,

$$\begin{aligned} & \{F_{1p}, e^{\epsilon_1^2 F_2} e^{\epsilon F_1} H_0\} = H_1 \\ \Rightarrow \quad & \{e^{-\epsilon_1 F_1} e^{-\epsilon_1^2 F_2} F_{1p}, H_0\} = e^{-\epsilon_1 F_1} e^{-\epsilon_1^2 F_2} H_1 \\ \Rightarrow \quad & F_{1p}(z) = e^{\epsilon_1^2 F_2} e^{\epsilon_1 F_1} \int_0^z e^{\tau H_0} e^{-\epsilon_1 F_1} e^{-\epsilon_1^2 F_2} H_1 d\tau + F_{1p}(0) \end{aligned}$$

The single step perturbation theory diverges if value of ϵ is beyond the radius of convergence but the two-step perturbation theory will give convergent results if the

two steps are correctly chosen. Inside the radius of convergence a third order single-step perturbation theory is supposed to give better results compared to a $(2 + 1)$ order two-step perturbation theory.

We applied the double-step perturbation theory to calculate the canonical transformation from $H_0 = \frac{p^2+q^2}{2}$ to $H = H_0 + \epsilon\frac{q^4}{4}$. The perturbed Hamiltonian H is one-degree-of-freedom and so it is integrable, further for positive values of ϵ the motion is compact for all energies. When ϵ is negative the motion for H become noncompact at large enough energy values. We calculated radius of convergence in ϵ in real time at the point $\epsilon = (0, 0)$ for specific initial conditions and applied the two-step theory taking both steps in ϵ to be positive so that the resulting system has compact dynamics. The results were compared at two different initial conditions and compared with the single-step theory results. Graph 3.1a shows constant of motion where the final ϵ lies outside the radius of convergence, plot $O(3)$ is the result of the single-step third order perturbation theory and $O(2 + 1)$ is the result of the two-step theory. Graph 3.1b is the same as graph 3.1a with the final ϵ being inside the radius of convergence.

As can be clearly seen from the graphs, In both the cases the third order predictions are better for time values which are well within the radius of convergence whereas the two-step perturbation theory results turn out to be better for larger time values. Graph 3.1a shows that when the radius of convergence is small the analytically continued generating function gives much better results than the single step theory.

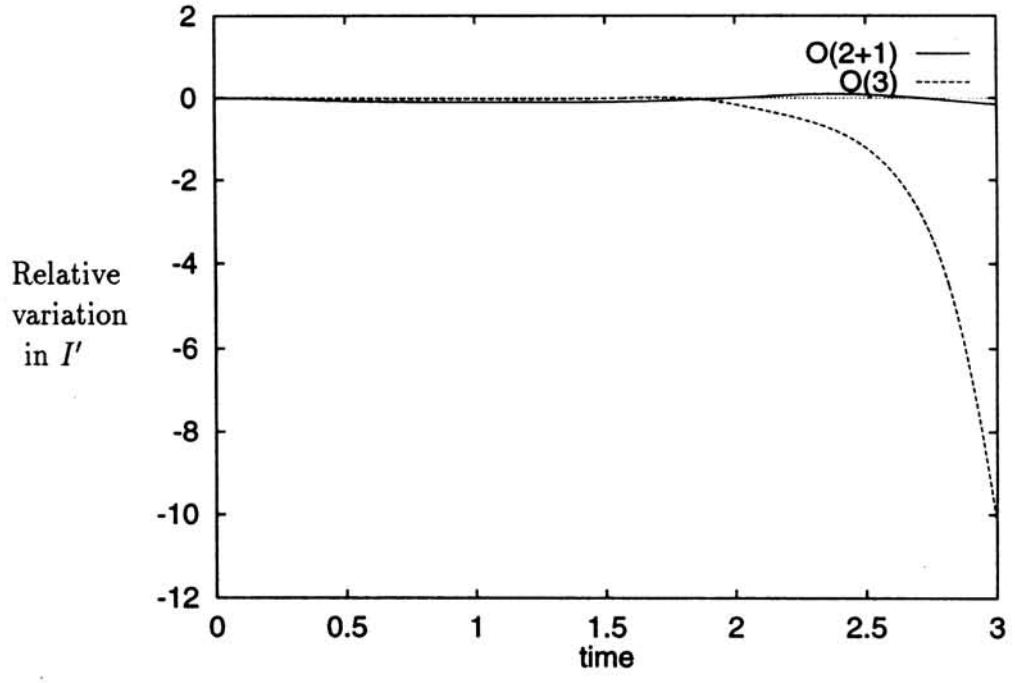

Graph: 3.1a: *Relative variation in predicted time-dependent constant of motion I'. The nearest singularity is at $t \simeq 2.67$. $O(2+1)$ shows the two-step perturbation theory results and $O(3)$ shows a single-step third order perturbation theory result.*

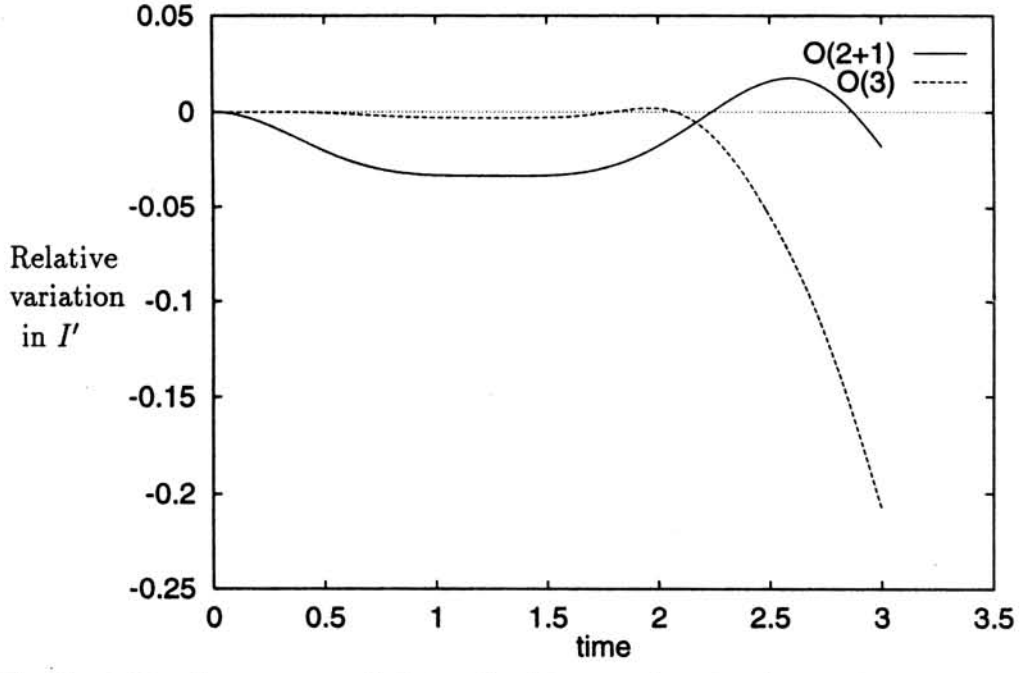

Graph: 3.1b: *Same as graph 3.1a, In this case the singularity is at* $t \simeq 9.63$

3.4 Exact Calculation of the TCPT for Some Special Cases

Though it is not possible to calculate the full TCPT transformation in general, for a class of perturbations where the resultant system are integrable, it is possible to calculate the total TCPT transformation.

Consider an integrable Hamiltonian H_0 which is perturbed by a constant perturbation H_1,

$$\{H_0, H_1\} = 0$$

Examples of such systems are where,
(1) H_1 is a function only of the unperturbed action variables,
(2) The angle dependence of H_1 is such that H_1 remains constant over unperturbed orbits.
In these cases only the first order generating function F_1 is non-zero, all the higher order generators vanish. This can be shown as follows. H_1 being constant on the unperturbed orbits means that $F_1 = \int H_1 d\tau = H_1 t$. Calculation of F_2 requires calculation of $\{F_1, \{F_1, H_0, \}\} = \{F_1, H_1\}$. Now $F_1 = H_1 t$ implies $\{F_1, H_1\} = 0$ which in turn implies $F_2 = 0$. In the same manner generators at all the orders are seen to be zero. In other words, because F_1 does not create terms of $O(\epsilon^2)$ or higher orders, there is no need to have higher order generating functions which were required to kill higher order terms in ϵ in the transformed Hamiltonian.

It should be noted that in both the above cases (1) and (2) the CPT is singular and so can not be applied. Now because in these cases only F_1 is nonzero and higher order generating function vanish, F_1 can be treated as the Hamiltonian for ϵ evolution. This follows from the fact that if the unperturbed Hamiltonian is considered to be $H_0 + \epsilon_1 H_1$ and the perturbation part, $\epsilon_2 H_1$, for all finite values of ϵ_1, F_1 remains the same. In other words at all values of ϵ,

$$\frac{dI_i}{d\epsilon} = \{I_i, F_1\}$$
$$\frac{d\theta_i}{d\epsilon} = \{\theta_i, F_1\}$$

which are the coefficients of the first order term in ϵ in the equations for mapping.

Let us consider an example where,

$$H_0 = I_1 + I_2\,; \;\; H_1 = 2\sqrt{I_1 I_2}\cos(\theta_1 - \theta_2)$$

It is easier to solve for the canonical transformation after the following coordinate change,

$$\begin{aligned} I_1 &\rightarrow \frac{p_1^2 + q_1^2}{2} \\ I_2 &\rightarrow \frac{p_2^2 + q_2^2}{2} \\ \theta_1 &\rightarrow \tan^{-1}\frac{-p_1}{q_1} \\ \theta_2 &\rightarrow \tan^{-1}\frac{-p_2}{q_2} \end{aligned}$$

under which the perturbed Hamiltonian becomes,

$$H = \frac{q_1^2 + q_2^2 + p_1^2 + p_2^2}{2} + \epsilon(q_1 q_2 + p_1 p_2)$$

Now,

$$F_1(t) = \int_0^t H_1(\phi + \omega(\tau - t), J, \tau)d\tau + F_1(0)$$

with $F_1(0) = 0$ and because H_1 is constant over unperturbed orbits,

$$F_1 = H_1 t = (q_1 q_2 + p_1 p_2)t$$

F_2 is calculated by integrating $-\frac{\{F_1, H_1\}}{2}$ over unperturbed orbits but $\{F_1, H_1\} = 0$, thus F_2 vanishes and similarly all the higher order generating functions also vanish. The equations defining the canonical transformation are,

$$\begin{aligned} \frac{dq_1}{d\epsilon} &= p_2 t \\ \frac{dq_2}{d\epsilon} &= p_1 t \\ \frac{dp_1}{d\epsilon} &= -q_2 t \\ \frac{dp_2}{d\epsilon} &= -q_1 t \end{aligned}$$

Which can be solved as,

$$\begin{aligned} q_1(\epsilon) &= q_{10}\cos\epsilon t + p_{20}\sin\epsilon t \\ q_2(\epsilon) &= q_{20}\cos\epsilon t + p_{10}\sin\epsilon t \\ p_1(\epsilon) &= -q_{20}\sin\epsilon t + p_{10}\cos\epsilon t \\ p_2(\epsilon) &= -q_{10}\sin\epsilon t + p_{20}\cos\epsilon t \end{aligned}$$

where q_{10} denotes solution of the q_1 equation at $\epsilon = 0$, i.e. the unperturbed solution etc.. It is straight-forward to see that these mapped solutions satisfy the differential equations given by the perturbed Hamiltonian system.

Chapter 4

Application of TCPT to the Henon-Heiles System

4.1 The Hamiltonian

The Henon-Heiles (H-H) system is a non-integrable Hamiltonian system which was first studied by Henon and Heiles [22] to investigate the integrability of the system describing the motion of a particle in an axisymmetric potential an example of which is the motion of a star in axisymmetric gravitational field. The Hamiltonian is given by,

$$H = \frac{p_1^2 + p_2^2 + q_1^2 + q_2^2}{2} + \epsilon(q_1^2 q_2 - \frac{q_2^3}{3}), \tag{4.1}$$

where ϵ is the perturbation parameter. This Hamiltonian can also be derived by truncating the Toda-lattice Hamiltonian which is for a system of three particles moving on a circle with exponential interactions,

$$H = \frac{P_1^2 + P_2^2 + P_3^2}{2} + e^{-(Q_1 - Q_3)} + e^{-(Q_2 - Q_1)} + e^{-(Q_3 - Q_2)} - 3 \tag{4.2}$$

truncating this Hamiltonian upto third order and applying a canonical transformation one gets the H-H Hamiltonian [3]. It is interesting to note that the Toda-lattice Hamiltonian is completely integrable whereas the H-H Hamiltonian is non-integrable. In fact truncation at different orders in the Toda-lattice Hamiltonian

gives a class of Hamiltonian systems, this class of Hamiltonian has been well-studied by Contopoulos and Polymilis [23]. The H-H Hamiltonian has also been studied extensively regarding the Painleve property and complex-time singularities of the solutions ([21],[7]).

One useful property of the H-H system is that the perturbation parameter ϵ can be scaled to one without changing the form of the Hamiltonian by following scaling transformation,

$$q_i \rightarrow \frac{Q_i}{\epsilon}$$

$$p_i \rightarrow \frac{P_i}{\epsilon}$$

$i = 1, 2$, under which,

$$H \rightarrow \frac{1}{\epsilon^2} h$$

where,

$$h = \frac{Q_1^2 + Q_2^2 + P_1^2 + P_2^2}{2} + Q_1^2 Q_2 - \frac{Q_2^3}{3}$$

thus solving for motion of Henon-Heiles system for one value of ϵ and different values of energy is equivalent to solving for one value of energy and different values of ϵ. Our approach here has been the first one i.e. we have fixed the value of ϵ to .01 and studied the system for different values of energy (energies are quoted for the equivalent Hamiltonian h, for comparison with other results).

The potential of the H-H is such that in a small region near origin it gives rise to a potential well, inside which the motion remain bounded but away from the origin the potential valley exists where the motion is unbounded. The critical value of the potential (and so the energy) upto which the motion is compact can be found by finding out the turning points of the potential, this critical energy E_c turns out to be $E_c = \frac{1}{6}$.

The H-H system shows a transition from regular behavior to chaotic behavior on the Poincare section with change in energy [3]. For $E < \frac{1}{12}$ the Poincare sections indicate regular motion, i.e. the section is filled with closed curves and there is no exponential divergence of the trajectories. In the range $\frac{1}{12} < E < \frac{1}{6}$ the motion shows a transition from regular to chaotic behavior, becoming more and more chaotic with

increase in E, i.e., the area which is covered by closed curves in the section becomes smaller with increase in E. Beyond $E = \frac{1}{6}$, the motion becomes non-compact, with solutions escaping to infinity. (There are unbounded orbits for all energies, including for those with $E < \frac{1}{6}$; these orbits do not play any role in our analysis, as a suitable choice of initial conditions ensures that the orbits remain bounded.)

Classical perturbation theory is known to be singular for this Hamiltonian because of resonances, which arise at second order in Perturbation theory.The KAM theorem cannot be applied directly to the system because the condition,

$$det(\frac{\partial \omega_i}{\partial I_j}) \neq 0$$

is not satisfied, as the unperturbed frequencies are independent of the actions. Gustavson's method give good results for small energies but does not predict the chaotic behavior of Poincare sections.

4.2 Generating Functions, Solutions and Invariants

We redefine the unperturbed Hamiltonian which is the harmonic oscillator Hamiltonian in the extended phase-space as,

$$H_0 \rightarrow \frac{p_1^2 + p_2^2 + q_1^2 + q_2^2}{2} + T \tag{4.3}$$

and the full Hamiltonian as,

$$H \rightarrow H_0 + \epsilon H_1 + T \tag{4.4}$$

where,

$$H_1 = q_1^2 q_2 - \frac{q_2^3}{3} \tag{4.5}$$

where (t, T) are extra phase space coordinates and the new Poisson bracket is redefined as,

$$\{f, g\} \rightarrow \frac{\partial f}{\partial t}\frac{\partial g}{\partial T} - \frac{\partial f}{\partial T}\frac{\partial g}{\partial t} + \{f, g\}$$

with $\{f, g\}$ denoting the usual Poisson bracket of f with g.

In unperturbed action-angle coordinates we get,

$$H_0 = I_1 + I_2 + T, \tag{4.6}$$

$$H_1 = 2I_1 \cos^2\theta_1 \sqrt{2I_2}\cos\theta_2 - \frac{(\sqrt{2I_2}\cos\theta_2)^3}{3} \tag{4.7}$$

The equations determining the generators are,

$$\{F_1, H_0\} = H_1 \tag{4.8}$$

$$\{F_2, H_0\} = -\frac{\{F_1, \{F_1, H_0\}\}}{2} \tag{4.9}$$

$$\{F_3, H_0\} = -\frac{\{F_1, \{F_1, \{F_1, H_0\}\}\}}{3!} - \{F_2, \{F_1, H_0\}\} \tag{4.10}$$

The F_i were calculated using Mathematica programs. The Mathematica program for calculation of the generating functions is given in the Appendix A-2 and the expression for the generating functions are given in the appendix A-3 to this chapter.

The constants of motion for H to third order are given by,

$$\begin{aligned} I_i' &= I_i + \epsilon\{F_1, I_i\} + \frac{\epsilon^2\{F_1, \{F_1, I_i\}\}}{2} + \frac{\epsilon^3\{F_1, \{F_1, \{F_1, I_i\}\}\}}{3!} \\ &+ \epsilon^2\{F_2, I_i\} + \epsilon^3\{F_2, \{F_1, I_i\}\} + \epsilon^3\{F_3, I_i\} \end{aligned} \tag{4.11}$$

where $i = 1, 2$.

The solutions of the EOM for H can be obtained from those of H_0 using the equations:

$$\begin{aligned} \xi_i &= \xi_i' - \epsilon\{F_1, \xi_i'\} + \epsilon^2\frac{\{F_1, \{F_1, \xi_i'\}\}}{2} - \epsilon^3\frac{\{F_1, \{F_1, \{F_1, \xi_i'\}\}\}}{3!} \\ &- \epsilon^2\{F_2, \xi_i'\} + \epsilon^3\{F_1, \{F_2, \xi_i'\}\} - \epsilon^3\{F_3, \xi_i'\} \end{aligned} \tag{4.12}$$

where $i = 1, 2, 3, 4$, $\xi_1 = I_1$, $\xi_2 = I_2$, $\xi_3 = \theta_1$, $\xi_4 = \theta_2$, $\xi_1' = I_1'$, $\xi_2' = I_2'$, $\xi_3' = \theta_1'$, $\xi_4' = \theta_2'$.

Here $I(t), \theta(t)$ represent the solutions of the EOM for the Henon-Heiles Hamiltonian, while $I'(t), \theta'(t)$ represent the solutions for the Harmonic Oscillator Hamiltonian.

4.3 Numerical Results

Using a 4^{th} order Runge-Kutta-Gill adaptive ODE solver, the EOM for the Henon-Heiles system were solved and the invariants predicted by third order Perturbation theory were computed. Following are the results;

Graph 4.1*a* and 4.1*b* give relative variation in one of the constants of motion (I_1') for two different energies. Energy for graph 4.1*a* is such that the perturbed motion is regular. Energy for graph 4.1*b* is above the energy for onset of chaos. In both the graphs results of the first, second and third order perturbation theory are shown which are denoted by O_1, O_2 and O_3 respectively. We have shown in the graphs the relative variation in $I_1'(t)$ which is calculated as $2(I_1'(t) - I_1'(0))/(I_1'(t) + I_1'(0))$. If the predicted constant were really a constant of motion the graph would have been the same as the x axes with the relative variation being zero all the time.Here because the perturbation theory has not been calculated exactly(and also because there are singularities in real time complex-ϵ space.) we do not get the expected result but it can be seen clearly that with increase in order of calculation the perturbation theory result limits to the expected result for small times.

Graph 4.2 shows the third order prediction of the constant of motion at different energy values, ranging from the regular (energy$< \frac{1}{12}$) to the chaotic regime (energy$> \frac{1}{12}$). With increase in energy the constancy becomes worse i.e. error increases but higher order results remain superior to lower order results for all energies for short time, at larger time the errors become too large because of explicit dependence on time and finite order calculation.

For computing the solutions, the same Runge-Kutta-Gill ODE solver was used and results were compared with the predictions of equations 4.12. These results are summarized in graphs 4.3*a* and 4.3*b* (solid lines), which show the relative error in predicted solutions with respect to numerical solutions; for the first, second and third order perturbation theory. The relative error in $I_1(t)$ is, $2(I_{1p}(t) - I_{1n}(t))/(I_{1p}(t) - I_{1n}(t))$, where I_{1p} is the predicted solution calculated using 4.12 and I_{1n} is the numerical solution calculated using Runge-Kutta algorithm. Graph 4.4 shows the mapping of solutions results of application of the third order perturbation theory

for a spectrum of energies ranging from the regular to the chaotic regime.

We also tested perturbation theory for two orbits of the Henon-Heiles system, one of which is known to be chaotic and the other regular (as seen from their Poincare sections). Graph 4.5*a* shows the behavior of the constants of motion for a chaotic trajectory and 5(*b*) shows the same for a regular trajectory, energy for both the orbits being the same. Graphs 4.6*a* and 4.6*b* are the Poincare sections for the initial conditions of 4.5*a* and 4.5*b* respectively. The Poincare section were computed in (p, q) coordinates, value of q_1 was set to zero and p_1 was required to be positive on intersection. (q_2, p_2) is the plane of the section shown. Following pages show the graphs.

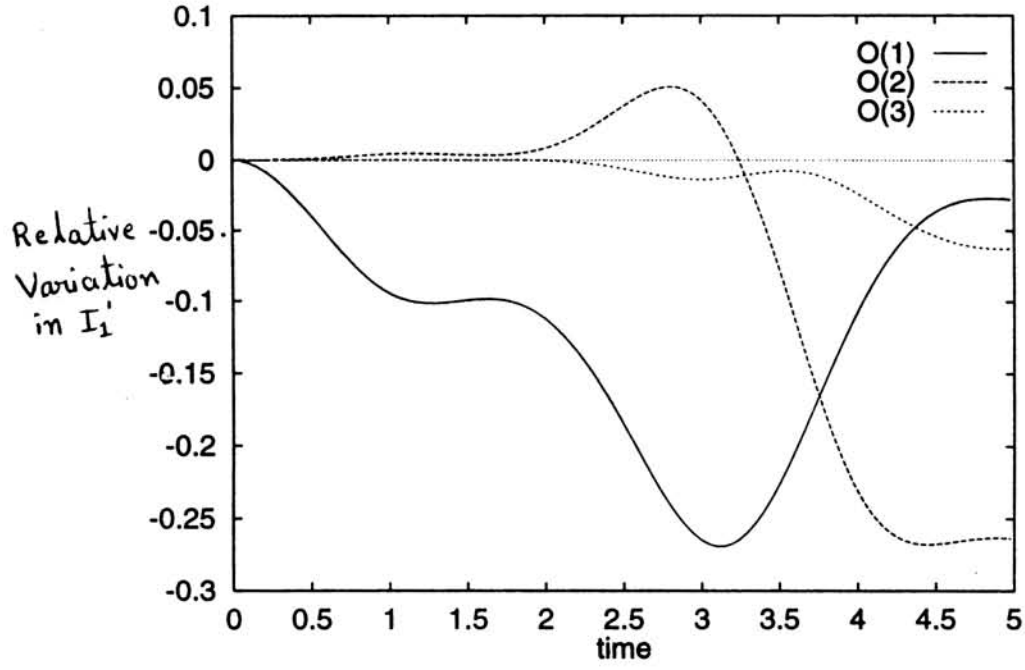

Graph 4.1a: *Relative variation in predicted time-dependent constant of motion* I_1' *for* $E = .034$. *O(1), O(2) and O(3) represent the first, second and third order perturbation theory results respectively.*

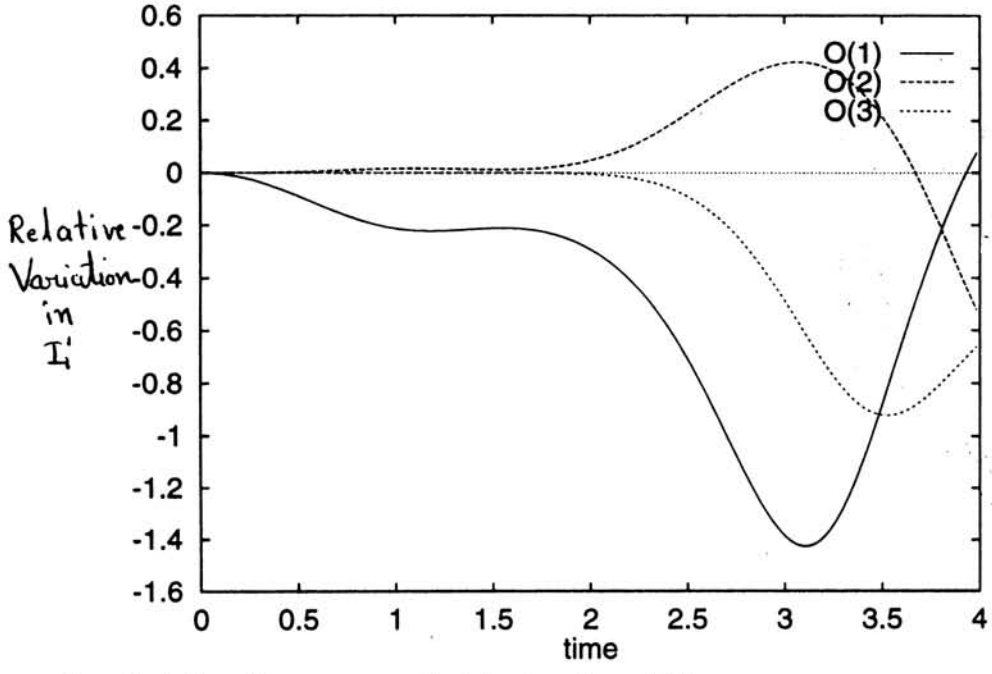

Graph 4.1b: *Same as graph 4.1a for* $E = .112$.

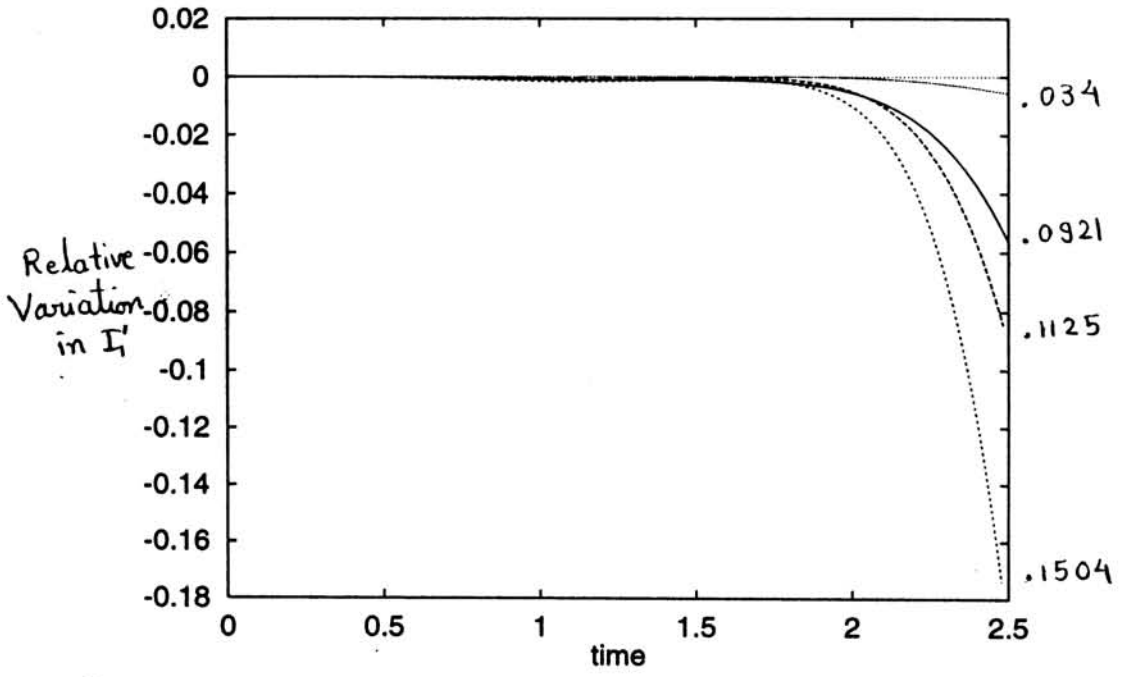

Graph 4.2: *Relative variation in predicted constant of motion at third order, at different E values for the Henon-Heiles system.*

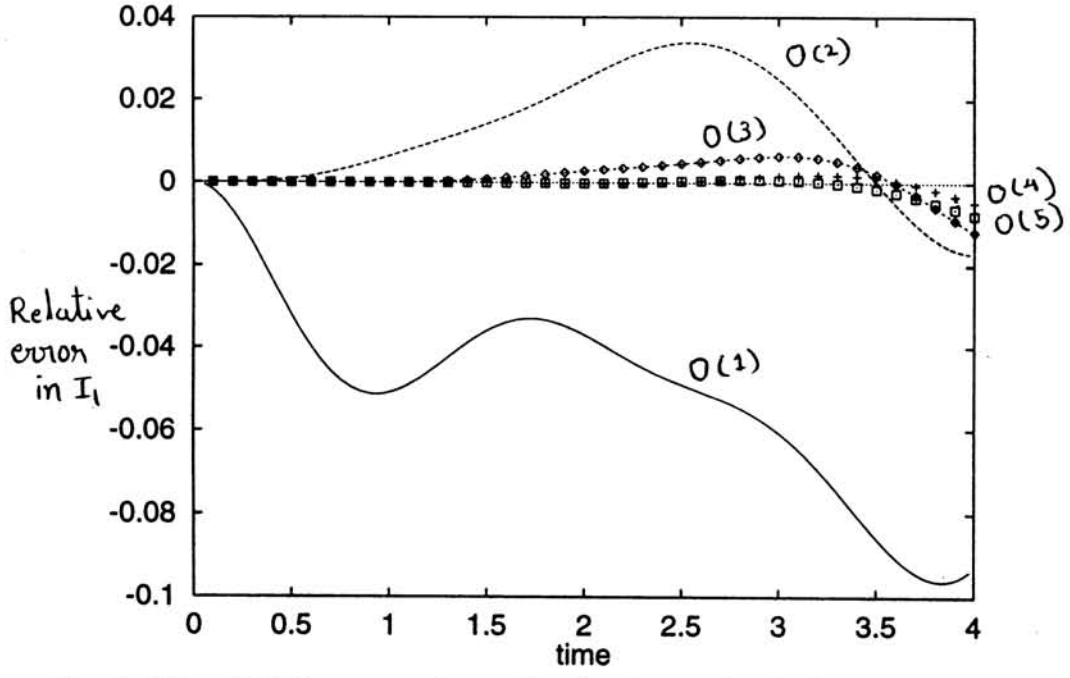

Graph 4.3a: *Relative error in predicted solution for I_1 for the Henon-Heiles system at $E = .034$. O(1),O(2) and O(3) represent the first, second and third order perturbation theory results respectively. Dotted curves show numerically calculated higher orders.*

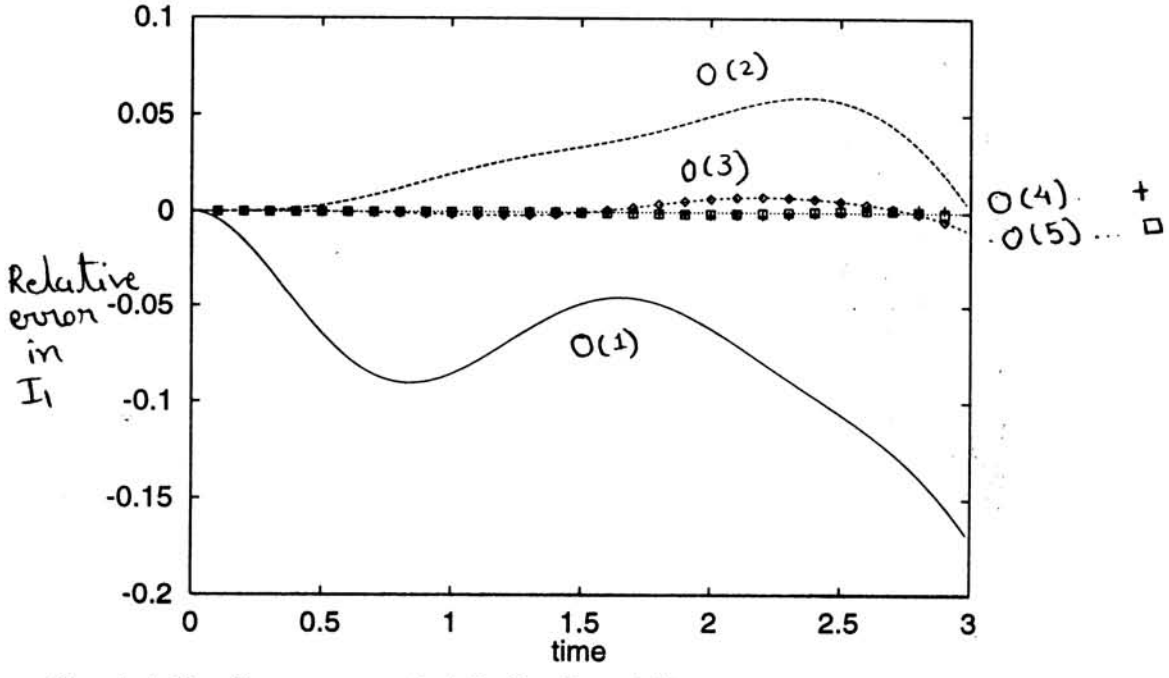

Graph 4.3b: *Same as graph 4.3a for $E = .112$.*

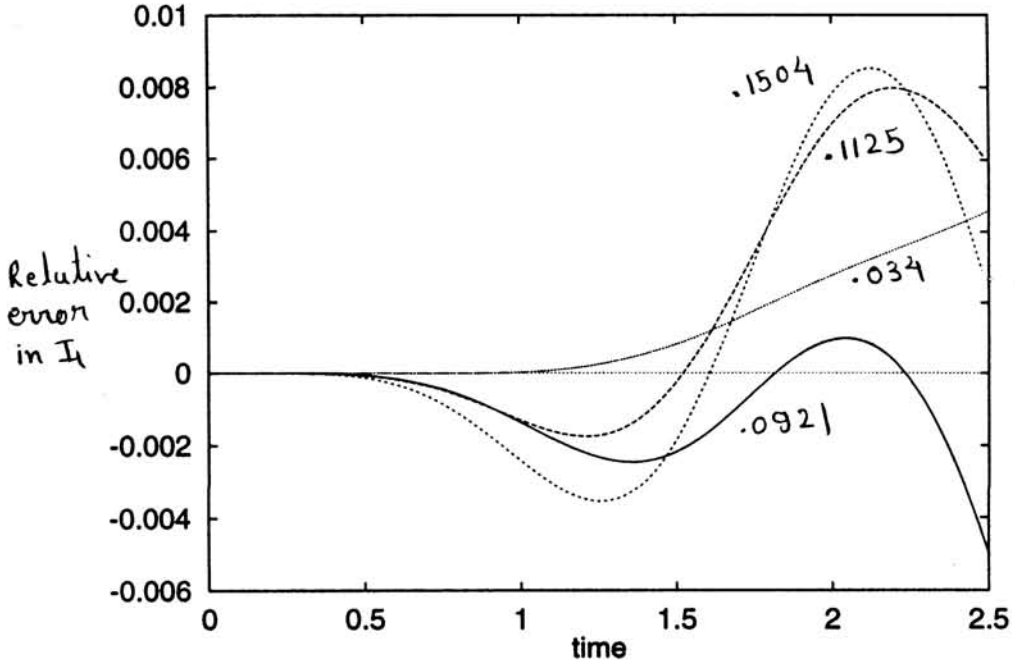

Graph 4.4: *Relative error in third order predicted solution for I_1 for the Henon-Heiles system at different energy values.*

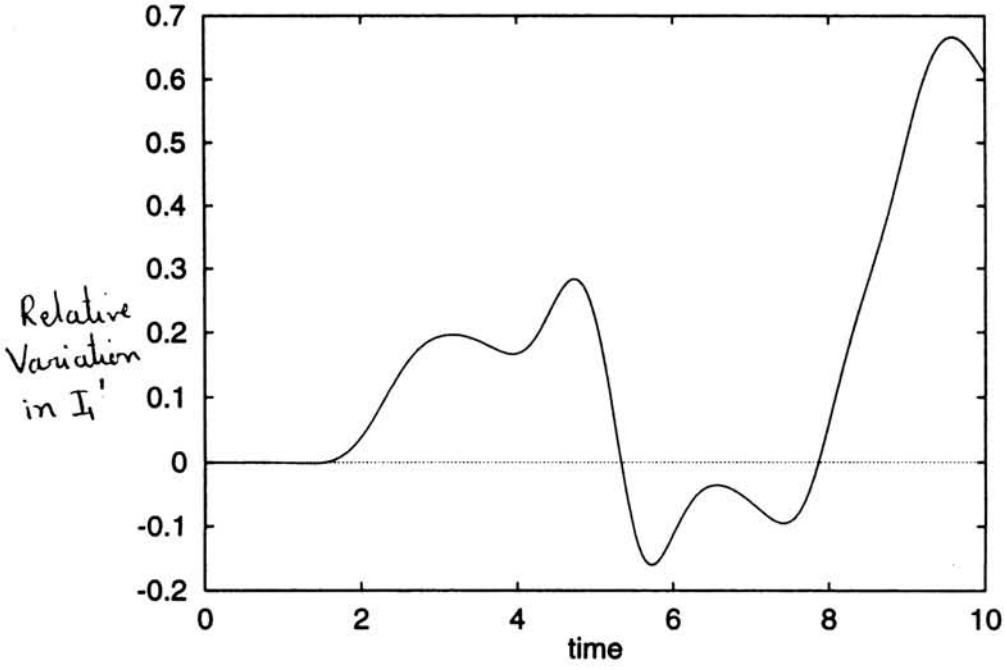

Graph 4.5a: *Relative variation in third order predicted constant of motion I_1' for the Henon-Heiles system for a chaotic orbit at $E = .125$.*

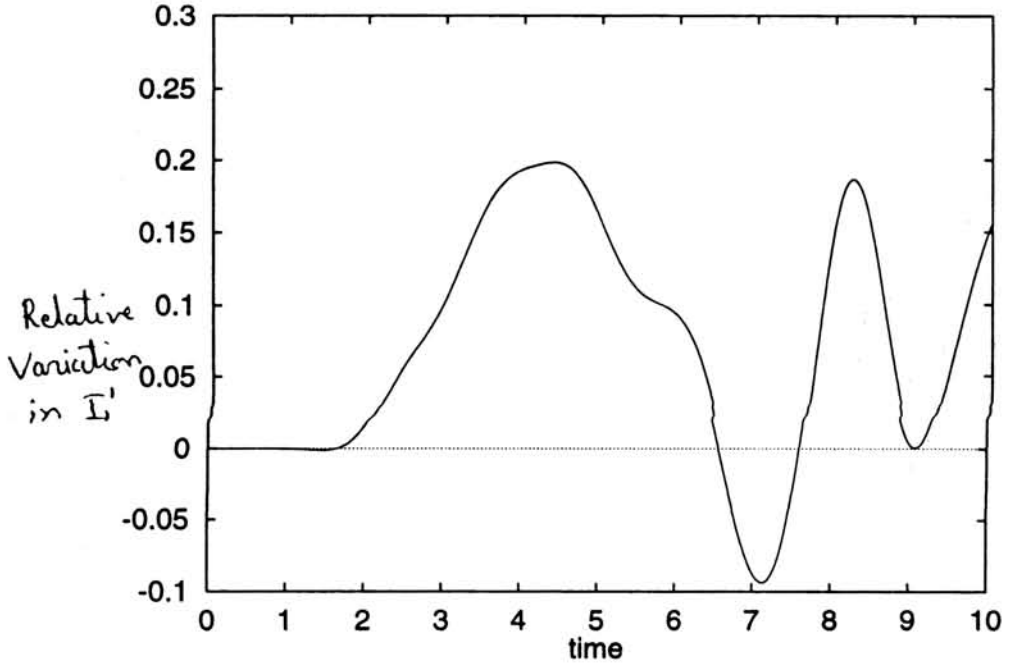

Graph 4.5b: *Same as in graph 4.5a for a regular orbit*

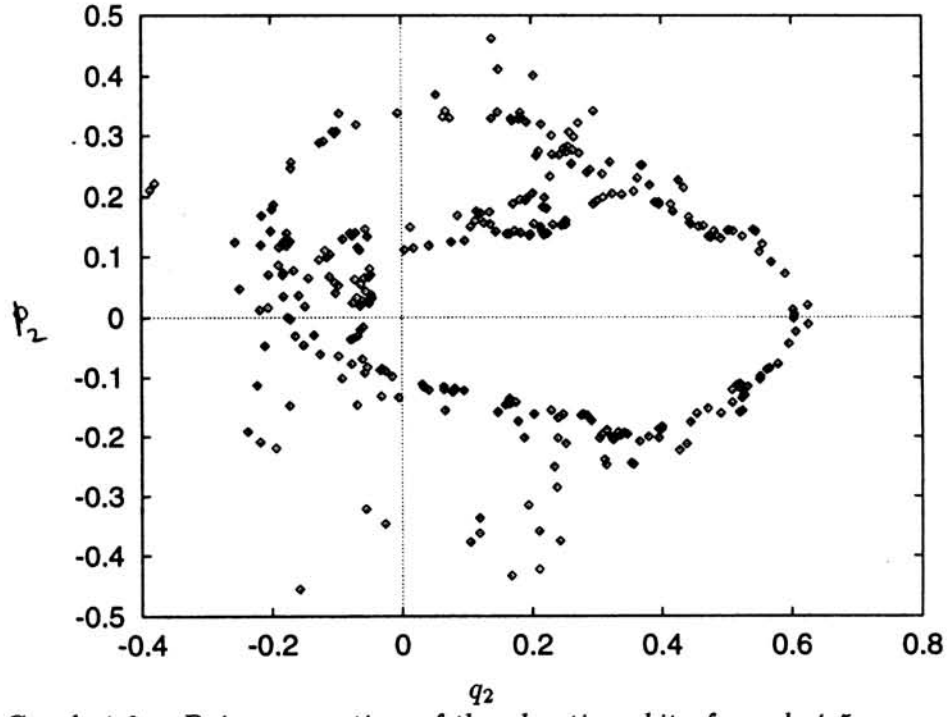

Graph 4.6a: *Poincare section of the chaotic orbit of graph 4.5a.*

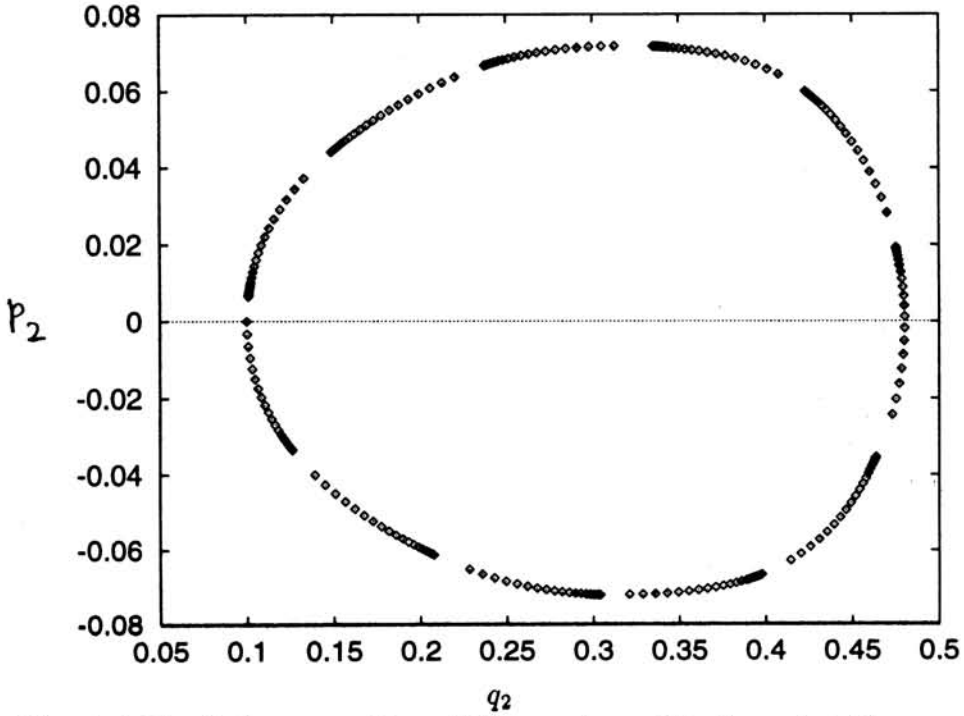

Graph 4.6b: *Poincare section of the regular orbit of graph 4.5b.*

4.4 Convergence of the Series

As it is obvious from the numerical results, the prediction of the perturbation theory does not seem to be in agreement with the numerical results for long time and high energies. This can be caused by two reasons,

1. Only first few orders of the perturbation series are considered, in which case the perturbation theory should agree with the numerical results at higher energies and larger times if enough number of terms in the perturbation series are considered.
2. Contrary to our assumption that the generating function is analytic in the complex ϵ plane, there exists a singularity; in that case one can expect the perturbation theory to converge only in the region where the distance of ϵ from origin is less than that of the radius of convergence.

To investigate which one of the former reasons is responsible for the disagreement of the perturbation theory with numerical calculations we analyzed the analytic structure of the system in complex ϵ real t space.

For the initial conditions selected for the graph 4.2, the equations were integrated in real time for 100 different ϵ values lying on a circle with radius .01 and center $\epsilon = (0, \vec{0})$. The failure of the integration subroutine was considered as existence of singularity. Three different subroutines drkgs(SSP; Runge-Kutta), d02baf(IMSL) and d02ebf(IMSL stiff equation solver) were used. Failure of d02ebf with ihalf = 2, was taken as presence of singularity. The results of the calculations are shown in table below. The smallest time at which one of the points on the circle becomes singular is given.

It is not expected that the above test will work for any general Hamiltonian because it does not detect branch point singularities, but in this specific case it turns out that a branch point in q_1 corresponds to a branch point in p_1 with negative exponent (this can be seen from Painleve analysis [7]) and same is true for q_2 and p_2. Thus eventhough there are singularities where the position variables remain finite, the corresponding momentum variables becomes infinite, hence the two type of singularities occur at the same time.

initial conditions				time for appearance of singularity		
q1	q2	p1	p2	drkgs	d02baf	d02ebf
4.4721	4.89898	0	0	$t > 200$	-	-
14.1421	21.4476	0	0	111.6145	$111.8 < t < 111.9$	$111.8 < t < 111.9$
30	24.4949	0	0	27.0544	$27.3 < t < 27.4$	$27.3 < t < 27.4$
29.6648	31.9374	0	0	19.37	$19.6 < t < 19.7$	$19.6 < t < 19.7$
34.9285	34.9285	0	0	13.4095	$13.6 < t < 13.7$	$13.6\ t < 13.7$

This analysis indicate that the perturbation theory should be convergent for given initial conditions and ϵ for larger time values than what is seen in the graph 4.2, thus the reason for disagreement should be truncation of the series rather than existence of a singularity. To verify this reasoning we did a numerical study as follows.

When one uses the generating functions for mapping of the solution for unperturbed Hamiltonian into the solution of the perturbed Hamiltonian, the result is the solution ξ of H in terms of solutions ξ' of H_0, t and a power series in ϵ. In this series for ξ the coefficient of a term ϵ^n is $\frac{1}{n!}\frac{d^n\xi}{d\epsilon^n}$. We did numerical calculations for $\frac{d^n\xi}{d\epsilon^n}$ using contour integral definition for derivatives and matched our numerical results with the analytical results predicted by perturbation theory. Details of this numerical calculation of the analytical prediction is given in appendix A-1. As can be seen from the graph 4.3, where the dotted curves denote numerically calculated higher orders, the third order analytical predictions are well in agreement with numerical values and the forth and fifth order numerical results shows that a higher order analytical calculation would make the predictions better.

To explain the worsening of perturbation theory at higher energies, we did the following calculation. We selected 100 different initial conditions randomly for each of 49 different energies and for each set of initial conditions we fixed 100 points on the complex ϵ circle with radius 1 and center (0,0) and calculated the minimum value of time at which one of the points on the circle became singular. This value of time is the minimum real time at which there is a singularity in the complex ϵ plane and this singularity will decide the radius of convergence for the perturbation theory. Graph 4.7 in next page shows the minimum and maximum value of the

above minimum time from the 100 initial conditions at each energy value. The minimum time value in the graph is the value upto which the perturbation theory will converge if enough number of orders are calculated, whereas the maximum at each energy shows that there are some initial conditions for which the perturbation theory will converge for very large time without any need for analytical continuation of the generator.

One important question is that what is the reason for reduction in radius of convergence with increase in energy ? It may be happening because of one or both of the following reasons, (1) The onset of chaos. (2) Approaching non-compact phase-space region. To test the second we applied TCPT to the anti-Henon-Heiles system defined by,

$$H_a = \frac{p_1^2 + p_2^2 + q_1^2 + q_2^2}{2} + \epsilon(q_1^2 q_2 + \frac{q_2^3}{3}) \tag{4.13}$$

This system is known to be integrable because it is separable under the canonical transformation,

$$q_1 \rightarrow \frac{x+y}{2} \quad q_2 \rightarrow \frac{x-y}{2}$$
$$p_1 \rightarrow \frac{p_x+p_y}{2} \quad p_2 \rightarrow \frac{p_x-p_y}{2}$$

For this system the motion becomes non-compact at energy$= \frac{1}{12\epsilon}$. The constants of motion calculation for H_a shown in graph 4.8 shows similar increase in errors as in Henon-Heiles, from which we conclude that non-compactness of motion also play a very important role in determining the behavior of the perturbation theory results.

It thus appears from our analysis that the time dependent canonical perturbation theory can be used for studying the Henon-Heiles system, the fact that the results show disagreement with numerical results is to be attributed to the low order of perturbation theory used.

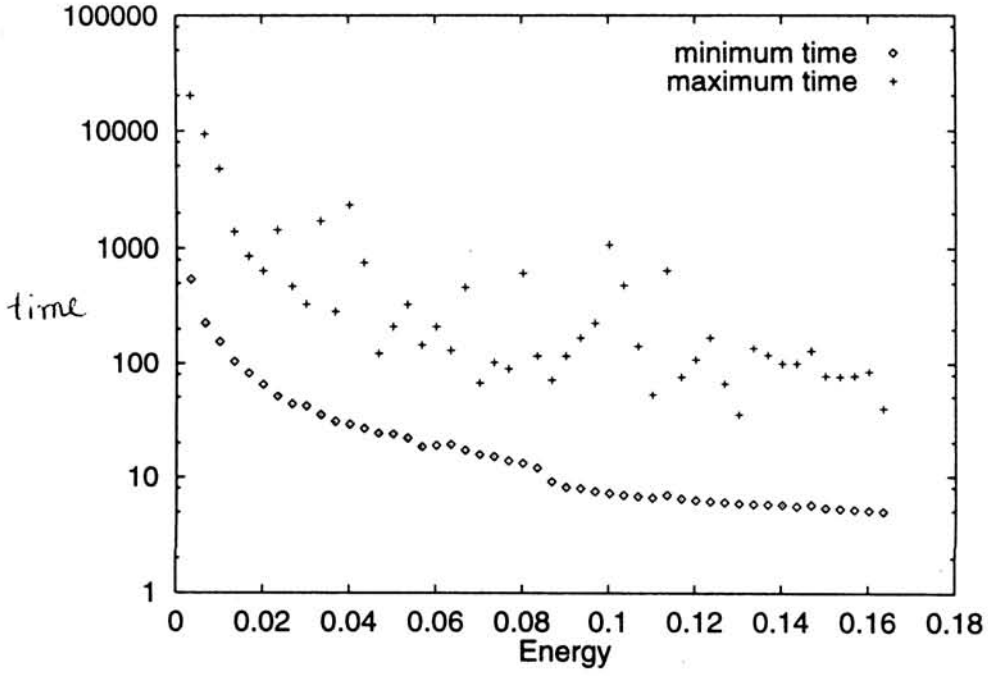

Graph 4.7: *At fixed energy 100 different initial conditions are chosen randomly and each initial conditions is evolved in time with all the 100 different ϵ values equally spaced on a circle of radius 1 and center $(0,0)$ in the complex-ϵ plane. The minimum time at which one of the points in complex-ϵ circle encounters a singularity is noted. From the minimum time thus found for each initial conditions at a fixed energy the minimum and maximum times are plotted against energy.*

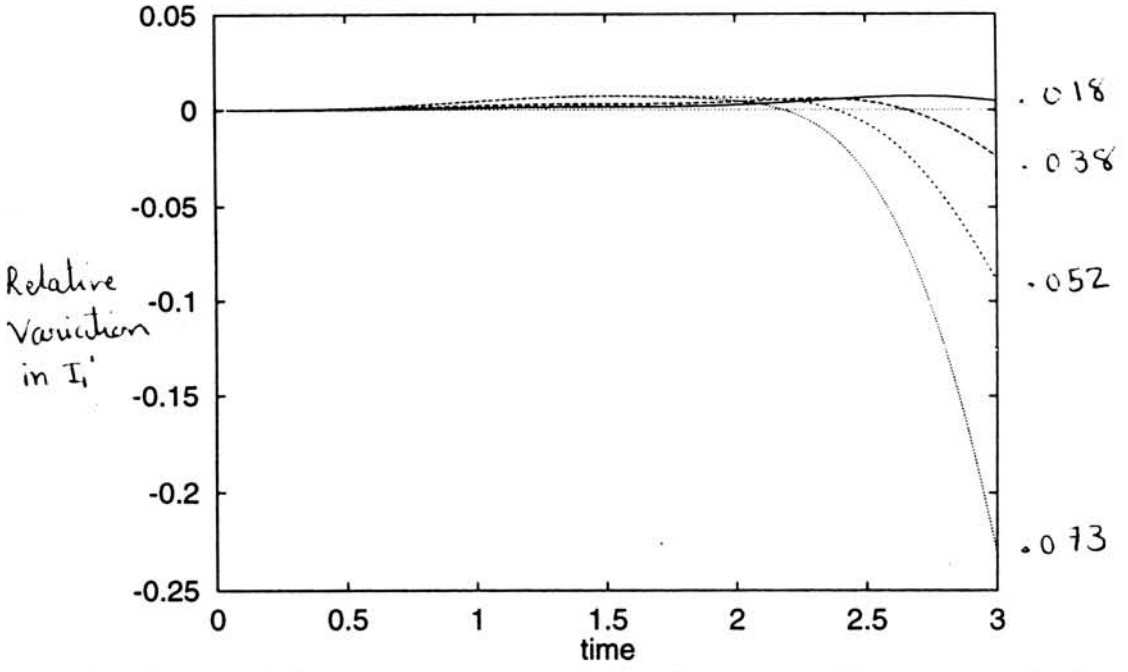

Graph 4.8: *Relative variation in predicted constant of motion at third order, at different E values for the anti-Henon-Heiles system.*

Appendix A-1: Numerical Calculation of Mapping

The mapping of solutions in TCPT is given by the following equation,

$$\begin{aligned}\xi_i &= \xi_i' - \epsilon\{F_1, \xi_i'\} + \epsilon^2 \frac{\{F_1, \{F_1, \xi_i'\}\}}{2} - \epsilon^3 \frac{\{F_1, \{F_1, \{F_1, \xi_i'\}\}\}}{3!} \\ &- \epsilon^2\{F_2, \xi_i'\} + \epsilon^3\{F_1, \{F_2, \xi_i'\}\} - \epsilon^3\{F_3, \xi_i'\}\end{aligned}$$

where $i = 1, 2, 3, 4$, $\xi_1 = I_1$, $\xi_2 = I_2$, $\xi_3 = \theta_1$, $\xi_4 = \theta_2$, $\xi_1' = I_1'$, $\xi_2' = I_2'$, $\xi_3' = \theta_2'$

Where $I(t)$, $\theta(t)$ represent the solutions of the EOM for the perturbed Hamiltonian, while $I'(t), \theta'(t)$ represent the solutions for the unperturbed Hamiltonian.

Thus the perturbed solution are written as a power series in ϵ. While compared with Taylor expansion in ϵ the term independent of ϵ in mapping equations is the perturbed solution at $\epsilon = 0$, i.e. the unperturbed solution. The coefficient of the the first order term in ϵ is the derivative of the perturbed solution evaluated at $\epsilon = 0$. The first order derivative can be evaluated as follows:

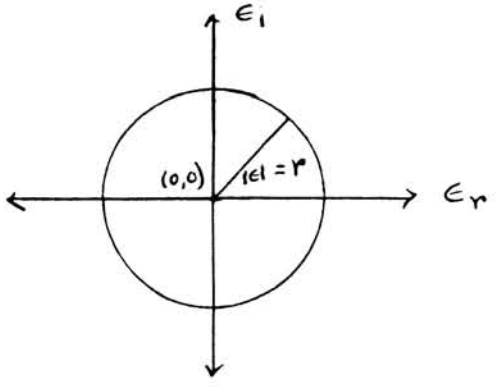

As shown in the figure around the point $\epsilon = (0, 0)$ in the complex plane values of ϵ were selected on a circular contour$|\epsilon| = r$. For given initial conditions the equations of motion can be solved with all these ϵ values upto time t of interest. Using these values the first order derivative of the perturbed solutions at the given time can be calculated using the following formula,

$$\left.\frac{d\xi_i(t)}{d\epsilon}\right|_{\epsilon=0} = \int_{contour} \frac{\xi_i(t)}{r} d\epsilon$$

where $\xi_i(t)$ as a function of ϵ has been calculated by numerically solving the equations of motion for different ϵ values. In the same manner all the higher order

coefficients of ϵ can be calculated numerically and thus one can predict the result of analytical calculation numerically. One efficint algorithm for numerical calculation of derivatives is described in [26], based on it's main idea our algorithm for numerical derivatives was written.

It is also possible to calculate the distance to the nearest singularity at a given time using the derivative ratios or other convergence tests proposed by Corliss and Chang [25]. We tried to calculate the radius of convergence using ration test as well as the three term test but because of requirement of calculation of very high order derivative and high precision our numerical method did not give convergent results.

Appendix A-2: Program for Calculation of Generating Functions

(* The Hamiltonian and the variables *)

$$
\begin{aligned}
q1 &= Sqrt[2 * i1] * Cos[theta1] \\
q2 &= Sqrt[2 * i2] * Cos[theta2] \\
p1 &= -Sqrt[2 * i1] * Sin[theta1] \\
p2 &= -Sqrt[2 * i2] * Sin[theta2] \\
h0 &= ExpandAll[p1^2/2 + p2^2/2 + q1^2/2 + q2^2/2 + T, Trig \rightarrow True] \\
h1 &= ExpandAll[q1^2 * q2 - q2^3/3, Trig \rightarrow True]
\end{aligned}
$$

(* The definition of a pb *)

$$
\begin{aligned}
pb[f\_, g\_] := \quad & D[f, theta1] * D[g, i1] - D[f, i1] * D[g, theta1] + \\
& D[f, theta2] * D[g, i2] - D[f, i2] * D[g, theta2] + \\
& D[f, t] * D[g, T] - D[f, T] * D[g, t]
\end{aligned}
$$

(* solving the perturbation equations *)

$$
\begin{aligned}
& solve1[rhs\_] := Integrate[rhs/.\{theta1 \rightarrow theta1 + tau - t, \\
& theta2 \rightarrow theta2 + tau - t, t \rightarrow tau\}, tau] \\
& solve[rhs\_] := \\
& Apply[Plus, Map[solve1, Apply[List, ExpandAll[rhs, Trig- > True]]]]
\end{aligned}
$$

(* Rules for Dt *)

$$
\begin{aligned}
& Unprotect[Dt] \\
& h = h0 + eps * h1 \\
& Dt[theta1, t] = D[h, i1] \\
& Dt[theta2, t] = D[h, i2] \\
& Dt[i1, t] = -D[h, theta1] \\
& Dt[i2, t] = -D[h, theta2] \\
& Dt[eps, t] = 0 \\
& Dt[T, t] = -D[h, t] \\
& Protect[Dt]
\end{aligned}
$$

$$
\begin{aligned}
o1 := Block\ [\ & \{\},\\
& f1h0 = h1;\\
& rhs1 = f1h0;\\
& f1 = solve[rhs1];\\
& f1 = (f1/.tau \to t) - (f1/.tau \to 0);\\
& f1 = ExpandAll[f1, Trig \to True]\\
&]
\end{aligned}
$$

$$
\begin{aligned}
o2 := Block\ [\ & \{\},\\
& f12h0 = pb[f1, f1h0];\\
& rhs2 = -f12h0/2;\\
& f2h0 = rhs2;\\
& f2 = solve[rhs2];\\
& f2 = (f2/.tau \to t) - (f2/.tau \to 0);\\
& f2 = ExpandAll[f2, Trig \to True]\\
&]
\end{aligned}
$$

$$
\begin{aligned}
o3 := Block\ [\ & \{\},\\
& f2f1h0 = pb[f2, f1h0];\\
& f13h0 = pb[f1, f12h0];\\
& rhs3 = -f13h0/6 - f2f1h0;\\
& f3h0 = rhs3;\\
& f3 = solve[rhs3];\\
& f3 = (f3/.tau \to t) - (f3/.tau \to 0);\\
& f3 = ExpandAll[f3, Trig- > True]\\
&]
\end{aligned}
$$

Appendix A-3: Expressions for The Generating Functions

We give below the form of the generating functions upto order ϵ^3.

$$
\begin{aligned}
F_1 &= \frac{-\left(I_2^{\frac{3}{2}}\sin(3t-3\theta_2)\right)}{9\sqrt{2}} + \sqrt{2}\,I_1\sqrt{I_2}\sin(t-\theta_2) \\
&- \frac{I_2^{\frac{3}{2}}\sin(t-\theta_2)}{\sqrt{2}} + \frac{I_1\sqrt{I_2}\sin(3t-2\theta_1-\theta_2)}{3\sqrt{2}} \\
&+ \frac{I_1\sqrt{I_2}\sin(2\theta_1-\theta_2)}{\sqrt{2}} + \sqrt{2}\,I_1\sqrt{I_2}\sin(\theta_2) \\
&- \frac{I_2^{\frac{3}{2}}\sin(\theta_2)}{\sqrt{2}} - \frac{I_2^{\frac{3}{2}}\sin(3\theta_2)}{9\sqrt{2}} \\
&+ \frac{I_1\sqrt{I_2}\sin(t-2\theta_1+\theta_2)}{\sqrt{2}} + \frac{I_1\sqrt{I_2}\sin(2\theta_1+\theta_2)}{3\sqrt{2}}
\end{aligned}
$$

$$
\begin{aligned}
F_2 &= \frac{-5\,{I_1}^2 t}{12} + \frac{I_1 I_2 t}{3} - \frac{5\,{I_2}^2 t}{12} - \frac{7\,I_1 I_2 t\cos(2\theta_1-2\theta_2)}{6} \\
&+ \frac{3\,{I_1}^2\sin(t)}{8} - \frac{I_1 I_2\sin(t)}{2} + \frac{3\,{I_2}^2\sin(t)}{8} + \frac{{I_1}^2\sin(3t)}{72} \\
&+ \frac{I_1 I_2\sin(3t)}{18} + \frac{{I_2}^2\sin(3t)}{72} + \frac{{I_1}^2\sin(t-4\theta_1)}{24} \\
&- \frac{{I_1}^2\sin(3t-4\theta_1)}{24} + \frac{{I_1}^2\sin(4t-4\theta_1)}{48} - \frac{{I_1}^2\sin(2t-2\theta_1)}{6} \\
&- \frac{I_1 I_2\sin(2t-2\theta_1)}{6} + \frac{{I_1}^2\sin(3t-2\theta_1)}{12} + \frac{I_1 I_2\sin(3t-2\theta_1)}{12} \\
&- \frac{{I_1}^2\sin(2\theta_1)}{6} - \frac{I_1 I_2\sin(2\theta_1)}{6} + \frac{{I_1}^2\sin(4\theta_1)}{48} \\
&+ \frac{{I_1}^2\sin(t+2\theta_1)}{12} + \frac{I_1 I_2\sin(t+2\theta_1)}{12} + \frac{{I_2}^2\sin(t-4\theta_2)}{24} \\
&- \frac{{I_2}^2\sin(3t-4\theta_2)}{24} + \frac{{I_2}^2\sin(4t-4\theta_2)}{48} - \frac{I_1 I_2\sin(2t-2\theta_2)}{6} \\
&- \frac{{I_2}^2\sin(2t-2\theta_2)}{6} + \frac{I_1 I_2\sin(3t-2\theta_2)}{12} + \frac{{I_2}^2\sin(3t-2\theta_2)}{12} \\
&+ \frac{I_1 I_2\sin(t-2\theta_1-2\theta_2)}{12} - \frac{I_1 I_2\sin(3t-2\theta_1-2\theta_2)}{12} \\
&+ \frac{I_1 I_2\sin(4t-2\theta_1-2\theta_2)}{24} + \frac{5\,I_1 I_2\sin(t+2\theta_1-2\theta_2)}{8}
\end{aligned}
$$

$$
\begin{aligned}
&- \frac{I_1 I_2 \sin(3t + 2\theta_1 - 2\theta_2)}{72} - \frac{I_1 I_2 \sin(2\theta_2)}{6} - \frac{{I_2}^2 \sin(2\theta_2)}{6} \\
&+ \frac{{I_2}^2 \sin(4\theta_2)}{48} + \frac{I_1 I_2 \sin(t + 2\theta_2)}{12} + \frac{{I_2}^2 \sin(t + 2\theta_2)}{12} \\
&+ \frac{5 I_1 I_2 \sin(t - 2\theta_1 + 2\theta_2)}{8} - \frac{I_1 I_2 \sin(3t - 2\theta_1 + 2\theta_2)}{72} \\
&+ \frac{I_1 I_2 \sin(2\theta_1 + 2\theta_2)}{24}
\end{aligned}
$$

$$
\begin{aligned}
\dot{F}_3 = \; & \frac{-7 I_1 {I_2}^{\frac{3}{2}} t \cos(2\theta_1 - 3\theta_2)}{2\sqrt{2}} - \frac{13 {I_1}^2 \sqrt{I_2}\, t \cos(2\theta_1 - \theta_2)}{3\sqrt{2}} \\
&+ \frac{37 I_1 {I_2}^{\frac{3}{2}} t \cos(2\theta_1 - \theta_2)}{6\sqrt{2}} - \frac{7 {I_1}^2 \sqrt{I_2}\, t \cos(4\theta_1 - \theta_2)}{18\sqrt{2}} \\
&+ \frac{11 {I_1}^2 \sqrt{I_2}\, t \cos(\theta_2)}{6\sqrt{2}} - \frac{13 I_1 {I_2}^{\frac{3}{2}} t \cos(\theta_2)}{3\sqrt{2}} \\
&+ \frac{5 {I_2}^{\frac{5}{2}} t \cos(\theta_2)}{6\sqrt{2}} - \frac{4\sqrt{2} I_1 {I_2}^{\frac{3}{2}} t \cos(3\theta_2)}{9} \\
&+ \frac{5 {I_2}^{\frac{5}{2}} t \cos(3\theta_2)}{18\sqrt{2}} - \frac{2\sqrt{2} {I_1}^2 \sqrt{I_2}\, t \cos(2\theta_1 + \theta_2)}{9} \\
&+ \frac{I_1 {I_2}^{\frac{3}{2}} t \cos(2\theta_1 + \theta_2)}{3\sqrt{2}} + \frac{{I_2}^{\frac{5}{2}} \sin(t - 5\theta_2)}{18\sqrt{2}} \\
&- \frac{{I_2}^{\frac{5}{2}} \sin(2t - 5\theta_2)}{216\sqrt{2}} - \frac{7 {I_2}^{\frac{5}{2}} \sin(3t - 5\theta_2)}{108\sqrt{2}} \\
&+ \frac{5 {I_2}^{\frac{5}{2}} \sin(4t - 5\theta_2)}{72\sqrt{2}} - \frac{2\sqrt{2} {I_2}^{\frac{5}{2}} \sin(5t - 5\theta_2)}{135} \\
&+ \frac{{I_2}^{\frac{5}{2}} \sin(6t - 5\theta_2)}{216\sqrt{2}} + \frac{5 I_1 {I_2}^{\frac{3}{2}} \sin(t - 3\theta_2)}{9\sqrt{2}} \\
&- \frac{7 {I_2}^{\frac{5}{2}} \sin(t - 3\theta_2)}{36\sqrt{2}} - \frac{I_1 {I_2}^{\frac{3}{2}} \sin(2t - 3\theta_2)}{18\sqrt{2}} \\
&- \frac{13 {I_2}^{\frac{5}{2}} \sin(2t - 3\theta_2)}{72\sqrt{2}} + \frac{\sqrt{2} I_1 {I_2}^{\frac{3}{2}} \sin(3t - 3\theta_2)}{27} \\
&+ \frac{5 {I_2}^{\frac{5}{2}} \sin(3t - 3\theta_2)}{27\sqrt{2}} - \frac{I_1 {I_2}^{\frac{3}{2}} \sin(4t - 3\theta_2)}{18\sqrt{2}} \\
&- \frac{{I_2}^{\frac{5}{2}} \sin(4t - 3\theta_2)}{18\sqrt{2}} + \frac{I_1 {I_2}^{\frac{3}{2}} \sin(6t - 3\theta_2)}{162\sqrt{2}} \\
&+ \frac{{I_2}^{\frac{5}{2}} \sin(6t - 3\theta_2)}{648\sqrt{2}} - \frac{I_1 {I_2}^{\frac{3}{2}} \sin(t - 2\theta_1 - 3\theta_2)}{9\sqrt{2}}
\end{aligned}
$$

$$
\begin{aligned}
&+ \frac{I_1 I_2^{\frac{3}{2}} \sin(2t - 2\theta_1 - 3\theta_2)}{108\sqrt{2}} + \frac{7 I_1 I_2^{\frac{3}{2}} \sin(3t - 2\theta_1 - 3\theta_2)}{54\sqrt{2}} \\
&- \frac{5 I_1 I_2^{\frac{3}{2}} \sin(4t - 2\theta_1 - 3\theta_2)}{36\sqrt{2}} + \frac{4\sqrt{2} I_1 I_2^{\frac{3}{2}} \sin(5t - 2\theta_1 - 3\theta_2)}{135} \\
&- \frac{I_1 I_2^{\frac{3}{2}} \sin(6t - 2\theta_1 - 3\theta_2)}{108\sqrt{2}} - \frac{355 I_1 I_2^{\frac{3}{2}} \sin(2\theta_1 - 3\theta_2)}{216\sqrt{2}} \\
&+ \frac{49\sqrt{2} I_1 I_2^{\frac{3}{2}} \sin(t + 2\theta_1 - 3\theta_2)}{27} - \frac{13 I_1 I_2^{\frac{3}{2}} \sin(2t + 2\theta_1 - 3\theta_2)}{18\sqrt{2}} \\
&- \frac{I_1 I_2^{\frac{3}{2}} \sin(3t + 2\theta_1 - 3\theta_2)}{54\sqrt{2}} + \frac{7 I_1 I_2^{\frac{3}{2}} \sin(4t + 2\theta_1 - 3\theta_2)}{216\sqrt{2}} \\
&- \frac{\sqrt{2} I_1^2 \sqrt{I_2} \sin(t - \theta_2)}{3} + \frac{23\sqrt{2} I_1 I_2^{\frac{3}{2}} \sin(t - \theta_2)}{9} \\
&- \frac{20\sqrt{2} I_2^{\frac{5}{2}} \sin(t - \theta_2)}{27} - \frac{I_1^2 \sqrt{I_2} \sin(2t - \theta_2)}{2\sqrt{2}} \\
&- \frac{2\sqrt{2} I_1 I_2^{\frac{3}{2}} \sin(2t - \theta_2)}{3} + \frac{11 I_2^{\frac{5}{2}} \sin(2t - \theta_2)}{18\sqrt{2}} \\
&+ \frac{5 I_1^2 \sqrt{I_2} \sin(3t - \theta_2)}{18\sqrt{2}} + \frac{I_1 I_2^{\frac{3}{2}} \sin(3t - \theta_2)}{9\sqrt{2}} \\
&- \frac{7 I_2^{\frac{5}{2}} \sin(3t - \theta_2)}{54\sqrt{2}} - \frac{I_1^2 \sqrt{I_2} \sin(4t - \theta_2)}{24\sqrt{2}} \\
&+ \frac{I_1 I_2^{\frac{3}{2}} \sin(4t - \theta_2)}{36\sqrt{2}} + \frac{I_2^{\frac{5}{2}} \sin(4t - \theta_2)}{216\sqrt{2}} \\
&- \frac{I_1^2 \sqrt{I_2} \sin(t - 4\theta_1 - \theta_2)}{6\sqrt{2}} + \frac{I_1^2 \sqrt{I_2} \sin(2t - 4\theta_1 - \theta_2)}{72\sqrt{2}} \\
&+ \frac{7 I_1^2 \sqrt{I_2} \sin(3t - 4\theta_1 - \theta_2)}{36\sqrt{2}} - \frac{5 I_1^2 \sqrt{I_2} \sin(4t - 4\theta_1 - \theta_2)}{24\sqrt{2}} \\
&+ \frac{2\sqrt{2} I_1^2 \sqrt{I_2} \sin(5t - 4\theta_1 - \theta_2)}{45} - \frac{I_1^2 \sqrt{I_2} \sin(6t - 4\theta_1 - \theta_2)}{72\sqrt{2}} \\
&+ \frac{I_1^2 \sqrt{I_2} \sin(t - 2\theta_1 - \theta_2)}{3\sqrt{2}} - \frac{I_1 I_2^{\frac{3}{2}} \sin(t - 2\theta_1 - \theta_2)}{6\sqrt{2}} \\
&+ \frac{I_1^2 \sqrt{I_2} \sin(2t - 2\theta_1 - \theta_2)}{2\sqrt{2}} + \frac{5 I_1 I_2^{\frac{3}{2}} \sin(2t - 2\theta_1 - \theta_2)}{12\sqrt{2}} \\
&- \frac{7\sqrt{2} I_1^2 \sqrt{I_2} \sin(3t - 2\theta_1 - \theta_2)}{27} - \frac{2\sqrt{2} I_1 I_2^{\frac{3}{2}} \sin(3t - 2\theta_1 - \theta_2)}{9}
\end{aligned}
$$

$$
\begin{aligned}
&+ \frac{{I_1}^2 \sqrt{I_2} \sin(4t - 2\theta_1 - \theta_2)}{6\sqrt{2}} + \frac{I_1 {I_2}^{\frac{3}{2}} \sin(4t - 2\theta_1 - \theta_2)}{6\sqrt{2}} \\
&- \frac{{I_1}^2 \sqrt{I_2} \sin(6t - 2\theta_1 - \theta_2)}{162\sqrt{2}} - \frac{I_1 {I_2}^{\frac{3}{2}} \sin(6t - 2\theta_1 - \theta_2)}{108\sqrt{2}} \\
&+ \frac{85 {I_1}^2 \sqrt{I_2} \sin(2\theta_1 - \theta_2)}{36\sqrt{2}} - \frac{185 I_1 {I_2}^{\frac{3}{2}} \sin(2\theta_1 - \theta_2)}{72\sqrt{2}} \\
&+ \frac{5 {I_1}^2 \sqrt{I_2} \sin(t + 2\theta_1 - \theta_2)}{3\sqrt{2}} - \frac{13 I_1 {I_2}^{\frac{3}{2}} \sin(t + 2\theta_1 - \theta_2)}{6\sqrt{2}} \\
&- \frac{{I_1}^2 \sqrt{I_2} \sin(2t + 2\theta_1 - \theta_2)}{9\sqrt{2}} - \frac{\sqrt{2} I_1 {I_2}^{\frac{3}{2}} \sin(2t + 2\theta_1 - \theta_2)}{9} \\
&+ \frac{I_1 {I_2}^{\frac{3}{2}} \sin(3t + 2\theta_1 - \theta_2)}{9\sqrt{2}} + \frac{5 {I_1}^2 \sqrt{I_2} \sin(4\theta_1 - \theta_2)}{54\sqrt{2}} \\
&+ \frac{{I_1}^2 \sqrt{I_2} \sin(t + 4\theta_1 - \theta_2)}{6\sqrt{2}} - \frac{{I_1}^2 \sqrt{I_2} \sin(3t + 4\theta_1 - \theta_2)}{324\sqrt{2}} \\
&- \frac{5 {I_1}^2 \sqrt{I_2} \sin(\theta_2)}{24\sqrt{2}} + \frac{85 I_1 {I_2}^{\frac{3}{2}} \sin(\theta_2)}{36\sqrt{2}} \\
&- \frac{155 {I_2}^{\frac{5}{2}} \sin(\theta_2)}{216\sqrt{2}} + \frac{5 I_1 {I_2}^{\frac{3}{2}} \sin(3\theta_2)}{54\sqrt{2}} \\
&- \frac{5 {I_2}^{\frac{5}{2}} \sin(3\theta_2)}{27\sqrt{2}} + \frac{43 {I_2}^{\frac{5}{2}} \sin(5\theta_2)}{1080\sqrt{2}} \\
&- \frac{{I_1}^2 \sqrt{I_2} \sin(t + \theta_2)}{2\sqrt{2}} + \frac{5 I_1 {I_2}^{\frac{3}{2}} \sin(t + \theta_2)}{3\sqrt{2}} \\
&- \frac{7 {I_2}^{\frac{5}{2}} \sin(t + \theta_2)}{18\sqrt{2}} - \frac{{I_1}^2 \sqrt{I_2} \sin(2t + \theta_2)}{3\sqrt{2}} \\
&- \frac{I_1 {I_2}^{\frac{3}{2}} \sin(2t + \theta_2)}{9\sqrt{2}} + \frac{2\sqrt{2} {I_2}^{\frac{5}{2}} \sin(2t + \theta_2)}{27} \\
&+ \frac{{I_1}^2 \sqrt{I_2} \sin(3t + \theta_2)}{9\sqrt{2}} - \frac{{I_2}^{\frac{5}{2}} \sin(3t + \theta_2)}{27\sqrt{2}} \\
&+ \frac{{I_1}^2 \sqrt{I_2} \sin(t - 4\theta_1 + \theta_2)}{4\sqrt{2}} + \frac{{I_1}^2 \sqrt{I_2} \sin(2t - 4\theta_1 + \theta_2)}{24\sqrt{2}} \\
&- \frac{{I_1}^2 \sqrt{I_2} \sin(3t - 4\theta_1 + \theta_2)}{27\sqrt{2}} + \frac{{I_1}^2 \sqrt{I_2} \sin(6t - 4\theta_1 + \theta_2)}{648\sqrt{2}} \\
&+ \frac{23\sqrt{2} {I_1}^2 \sqrt{I_2} \sin(t - 2\theta_1 + \theta_2)}{9} - \frac{26\sqrt{2} I_1 {I_2}^{\frac{3}{2}} \sin(t - 2\theta_1 + \theta_2)}{9}
\end{aligned}
$$

$$
\begin{aligned}
&- \frac{2\sqrt{2}\,{I_1}^2\sqrt{I_2}\,\sin(2t-2\theta_1+\theta_2)}{3} + \frac{5\,I_1\,{I_2}^{\frac{3}{2}}\,\sin(2t-2\theta_1+\theta_2)}{6\sqrt{2}} \\
&+ \frac{{I_1}^2\sqrt{I_2}\,\sin(3t-2\theta_1+\theta_2)}{9\sqrt{2}} + \frac{I_1\,{I_2}^{\frac{3}{2}}\,\sin(3t-2\theta_1+\theta_2)}{6\sqrt{2}} \\
&+ \frac{{I_1}^2\sqrt{I_2}\,\sin(4t-2\theta_1+\theta_2)}{36\sqrt{2}} - \frac{5\,I_1\,{I_2}^{\frac{3}{2}}\,\sin(4t-2\theta_1+\theta_2)}{72\sqrt{2}} \\
&+ \frac{25\,{I_1}^2\sqrt{I_2}\,\sin(2\theta_1+\theta_2)}{54\sqrt{2}} + \frac{5\,I_1\,{I_2}^{\frac{3}{2}}\,\sin(2\theta_1+\theta_2)}{18\sqrt{2}} \\
&- \frac{I_1\,{I_2}^{\frac{3}{2}}\,\sin(t+2\theta_1+\theta_2)}{3\sqrt{2}} + \frac{{I_1}^2\sqrt{I_2}\,\sin(3t+2\theta_1+\theta_2)}{81\sqrt{2}} \\
&+ \frac{I_1\,{I_2}^{\frac{3}{2}}\,\sin(3t+2\theta_1+\theta_2)}{54\sqrt{2}} - \frac{43\,{I_1}^2\sqrt{I_2}\,\sin(4\theta_1+\theta_2)}{360\sqrt{2}} \\
&+ \frac{{I_1}^2\sqrt{I_2}\,\sin(t+4\theta_1+\theta_2)}{36\sqrt{2}} + \frac{2\sqrt{2}\,I_1\,{I_2}^{\frac{3}{2}}\,\sin(t+3\theta_2)}{9} \\
&- \frac{{I_2}^{\frac{5}{2}}\,\sin(t+3\theta_2)}{18\sqrt{2}} - \frac{I_1\,{I_2}^{\frac{3}{2}}\,\sin(3t+3\theta_2)}{81\sqrt{2}} \\
&- \frac{{I_2}^{\frac{5}{2}}\,\sin(3t+3\theta_2)}{324\sqrt{2}} + \frac{23\,I_1\,{I_2}^{\frac{3}{2}}\,\sin(t-2\theta_1+3\theta_2)}{18\sqrt{2}} \\
&+ \frac{I_1\,{I_2}^{\frac{3}{2}}\,\sin(2t-2\theta_1+3\theta_2)}{27\sqrt{2}} - \frac{I_1\,{I_2}^{\frac{3}{2}}\,\sin(3t-2\theta_1+3\theta_2)}{27\sqrt{2}} \\
&- \frac{43\,I_1\,{I_2}^{\frac{3}{2}}\,\sin(2\theta_1+3\theta_2)}{540\sqrt{2}} + \frac{I_1\,{I_2}^{\frac{3}{2}}\,\sin(t+2\theta_1+3\theta_2)}{54\sqrt{2}} \\
&- \frac{{I_2}^{\frac{5}{2}}\,\sin(t+5\theta_2)}{108\sqrt{2}}
\end{aligned}
$$

Chapter 5

Application of TCPT to a KAM-type System

In chapter 4 we discussed application of TCPT to the Henon- -Heiles Hamiltonian, for which the unperturbed frequencies are independent of phase-space variables, because of which KAM theorem can not be applied to this system. Application of KAM theorem requires the unperturbed frequencies to be non-degenerate, i.e.,

$$det(\frac{\partial \omega_i}{\partial I_j}) \neq 0$$

in this chapter we shall consider a Hamiltonian system for which the unperturbed frequencies are non-degenerate and apply TCPT to it.

5.1 The Hamiltonian

The Hamiltonian considered is,

$$H(I_1, I_2, \theta_1, \theta_2) = \frac{I_1^2}{2} + \frac{I_2^2}{2} + \epsilon(I_1 Cos\theta_2 + I_2 Cos\theta_1) \tag{5.1}$$

This Hamiltonian was chosen because,
1. It is a Hamiltonian on which KAM theory can be applied.
2. The simplicity of the solutions of unperturbed equations of motion makes the application of TCPT simpler.

Non-degeneracy of the unperturbed frequencies can be easily seen as follows. The unperturbed frequencies for coordinates θ_1 and θ_2 are I_1 and I_2 respectively. The following condition is satisfied everywhere on the phase-space,

$$det(\frac{\partial \omega_i}{\partial I_j}) = 1$$

thus frequencies are functionally independent everywhere on the phase-space and so KAM theorem can be applied.

Usually integrable Hamiltonian systems with phase-space dependent frequencies have solutions which are Jacobi Elliptic or related functions of time. TCPT requires integration over unperturbed trajectories for calculation of generating function. It is very difficult to integrate products of above mentioned function analytically, further one expects the expressions of the integrand to become clumsier at each order of the perturbation theory. The Hamiltonian selected has the advantage that the unperturbed solutions are very simple and so choice of this Hamiltonain makes the application of TCPT simpler.

Poincare sections for the system shows the Hamiltonian to be non-integrable. As can be seen from the poincare section of graph 5.1a and 5.1b, chaotic and regular orbits coexist at energy= 2.0 and $\epsilon = .15$. Graph 5.2 shows a chain of island at the same energy. Ergodicity on phase-space increases with increase in the perturbation parameter while energy is fixed or equivalently with decrease in energy with perturbation parameter ϵ fixed. The equivalence of increase in ϵ with decrease in energy comes from the scaling property of the Hamiltonian with which one can transform Hamiltonian with a given perturbation parameter to the Hamiltonian with $\epsilon = 1$, with corresponding scaling in energy.The scaling equations are,

$$\theta_i \rightarrow \phi_i$$

$$I_i \rightarrow J_i \epsilon$$

which yields,

$$H = \epsilon^2 h \tag{5.2}$$

where,

$$h(J_1, J_2, \phi_1, \phi_2) = \frac{J_1^2}{2} + \frac{J_2^2}{2}(J_1 Cos\phi_2 + J_2 Cos\phi_1) \tag{5.3}$$

Thus as we had seen in the case of the Henon-Heiles Hamiltonian, existence of natural boundary in complex time for the system implies existence of natural boundary in complex ϵ plane for fixed real time, also studying the system at a fixed energy and different ϵ values is equivalent to studying the system at a fixed ϵ value and different energies.

5.2 Numerical Results

We used Mathematica programs for calculation of the generating functions, invariants and mapping results. All calculation were done with $\epsilon = .15$. There are terms in the generator and the invariants with denominators of the form $(n \cdot \omega)$ and its powers, which vanish in certain regions of phase-space. These singularities which are also known as the resonant terms arise because the canonical transformation being calculated is ill-defined. The apparent singularities (resonant terms) can be removed by making the canonical transformation time-dependent and taking the limit $(n \cdot \omega) \rightarrow 0$ in the region of phase-space where the usual generating function is singular. The limit turns out to be finite as can be seen from expressions for the first two order calculation of the generating function and two of their limits given in appendix B. The limit calculations were also done on Mathematica. The expressions for invariants and mapping of solutions upto n^{th} order are given by the following formulae. For invariants I_i',

$$I_i' = e^{\epsilon^n F_n} \ldots e^{\epsilon F_1} I_i \tag{5.4}$$

where I_i represent solutions for equations of motion for H. Mapping from solutions ξ_i' of H_0 to solutions ξ_i of H is given by,

$$\xi_i = e^{-\epsilon F_1} e^{-\epsilon^2 F_2} \ldots e^{-\epsilon^n F_n} \xi_i' \tag{5.5}$$

For the calculation of invariants a Runge-Kutta fourth order algorithm was used. Graph 5.1a and 5.1b show Poincare sections of a chaotic and a regular orbit respectively at the same energy, energy = 2.0 ($\epsilon = .15$). Graph 5.2 shows a chain of island at the same energy. Graph 5.3a shows the relative variation in I_1' for the chaotic orbit of graph 5.1a (the relative variation is defined as $2*(I_1'(t)-I_1'(0))/(I_1'(t)+I_1'(0))$. Graph 5.3b shows the same for the regular orbit of graph 5.1b. Graph 5.4a shows mapping of solution for chaotic orbit of graph 5.1a, the connected line is the relative error in mapped solution with respect to numerically calculated exact solution at first order of calculation, the dotted curves shows the relative error at higher orders. (The relative error in mapping is defined as $2(I_{1p}(t) - I_{1n}(t))/(I_{1p}(t) - I_{1n}(t))$ where I_{1p} is the predicted solution and I_{1n} is the numerical solution.) Graph 5.4b is the same as 5.4a for the regular orbit of graph 5.1b. Calculation for mapping at higher orders (shown by dotted curves in the graph) was done numerically using a program that calculates derivatives of the perturbed solution with respect to ϵ at $\epsilon = 0$ at given time and initial conditions. The program has been discussed in appendix A-1 of chapter-4. Both the invariant and the mapping errors decrease with increase in order of the calculation.

We also calculated position of blowing-up singularities (where solutions become infinite) in complex ϵ plane for real time, which gives the radius of convergence of the perturbation series in ϵ if there are no other finite singularities (where solutions have finite values). The NAG program d02baf was used with 256 points equally spaced on a circle with center $(0,0)$ and radius 0.15 in complex-ϵ plane, to get evolution of given initial conditions in real time and to find the smallest value of time at which one of the points on the circle has a blowing-up solution. The initial conditions of graph 5.2a has a singularity at $t \simeq 22.6$ and for graph 5.2b there is a singularity at $t \simeq 11.3$.

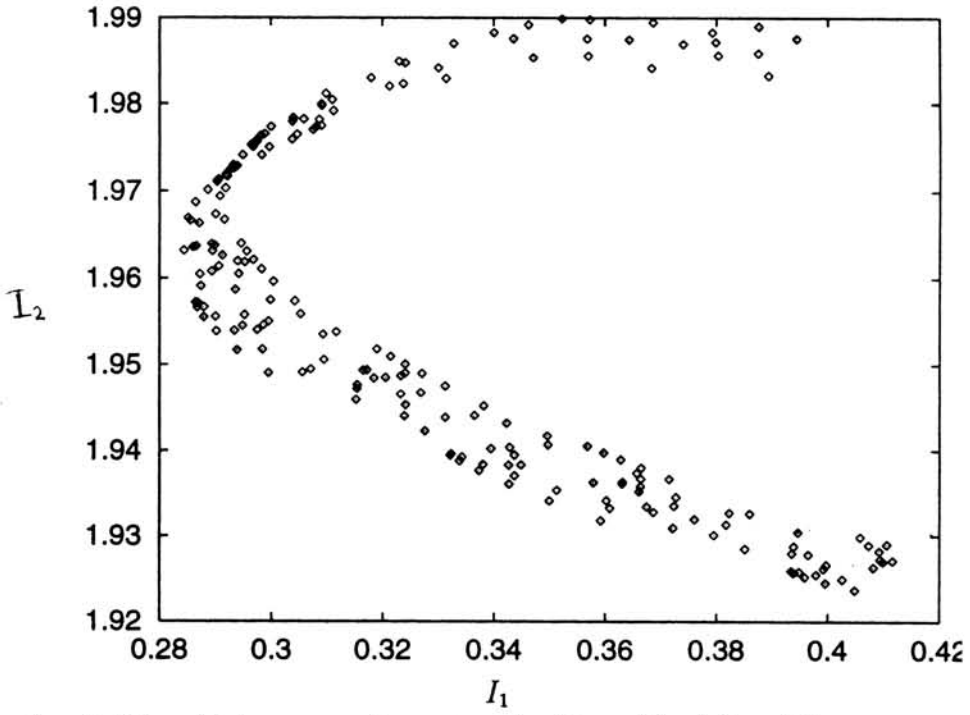

Graph 5.1a: *Poincare section of a chaotic orbit at* $E = 2.0$.

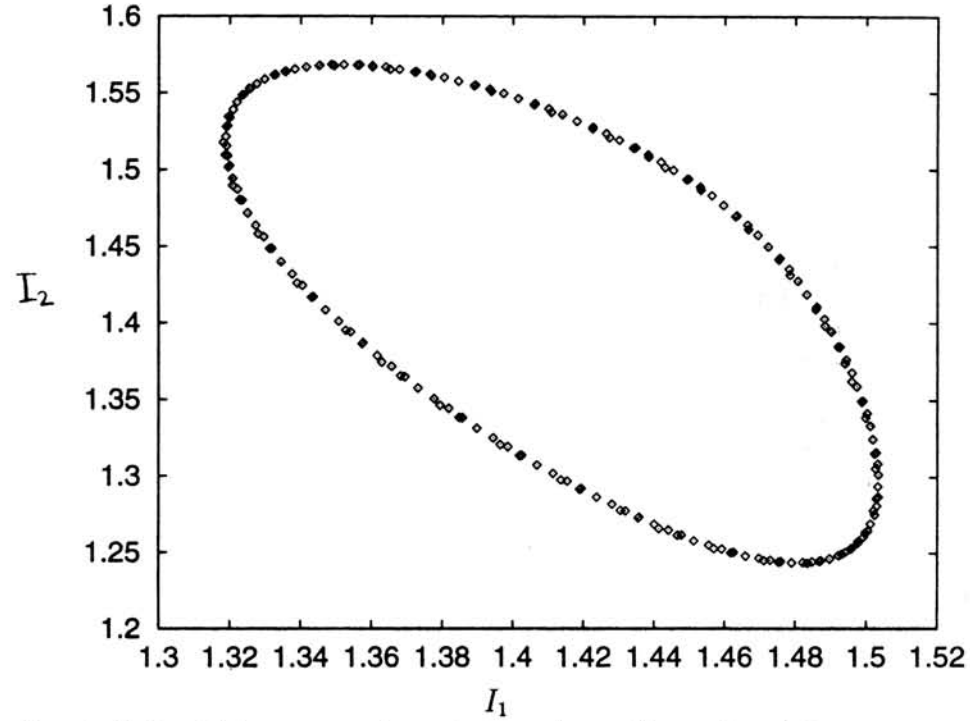

Graph 5.1b: *Poincare section of a regular orbit at* $E = 2.0$.

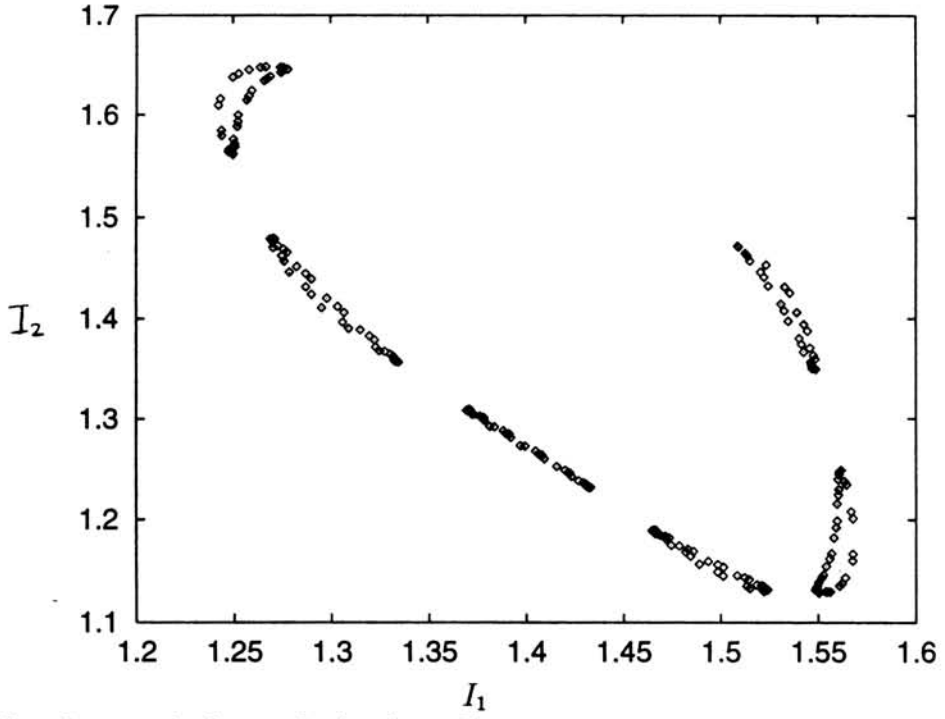

Graph 5.2: *A chain of islands at* $E = 2.0$.

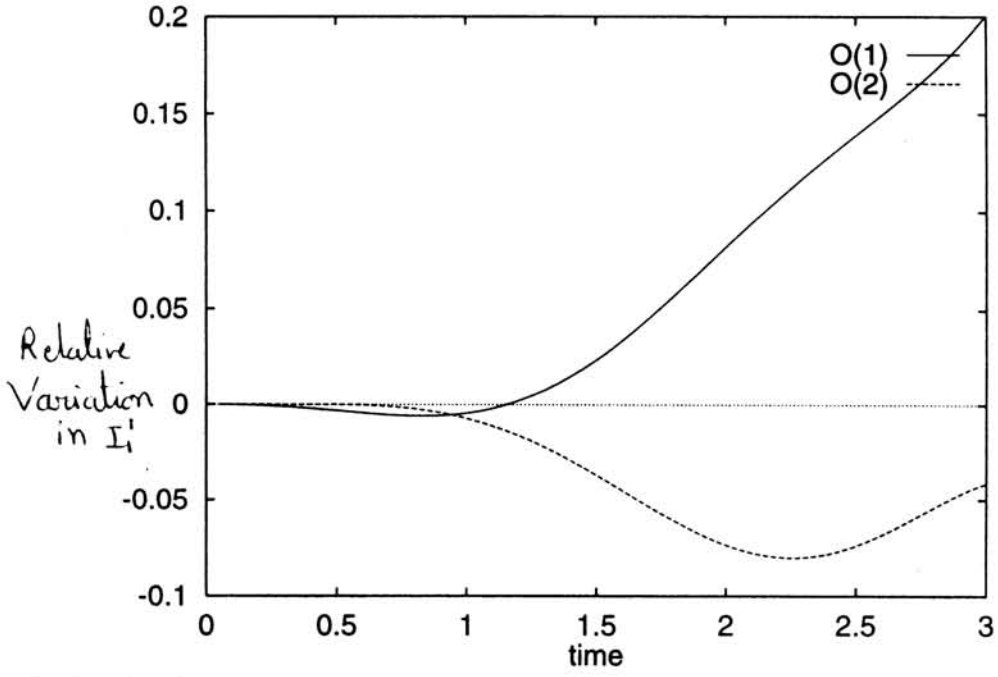

Graph 5.3a: *Relative variation in I_1' for the chaotic orbit of graph 5.1a. $O(1)$ and $O(2)$ shows first and second order perturbation theory results respectively.*

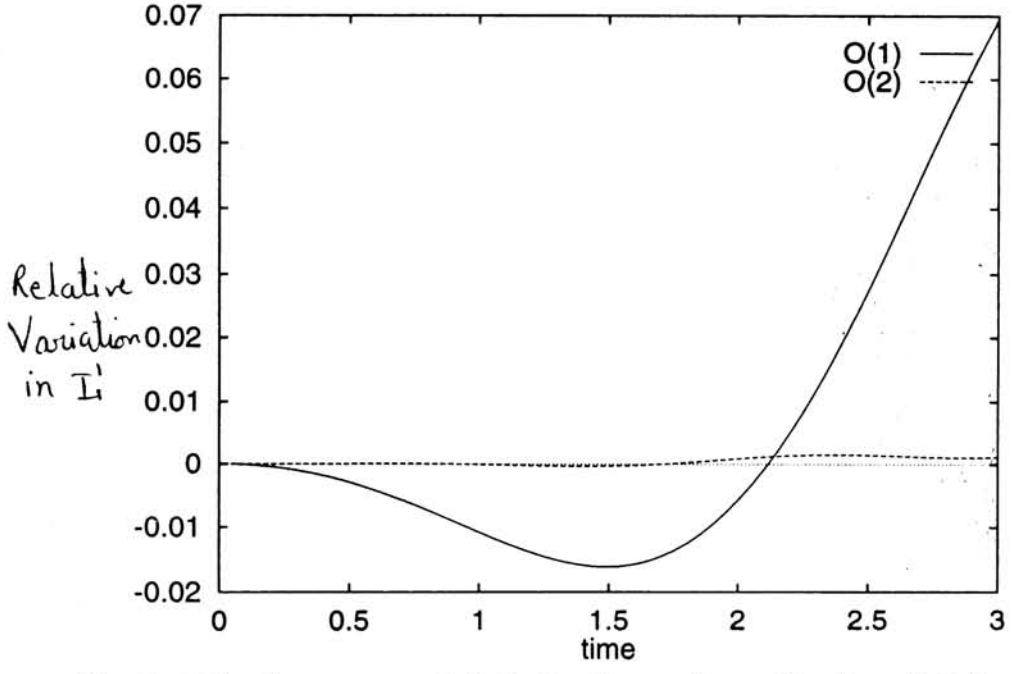

Graph 5.3b: *Same as graph 5.3a for the regular orbit of graph 5.1b.*

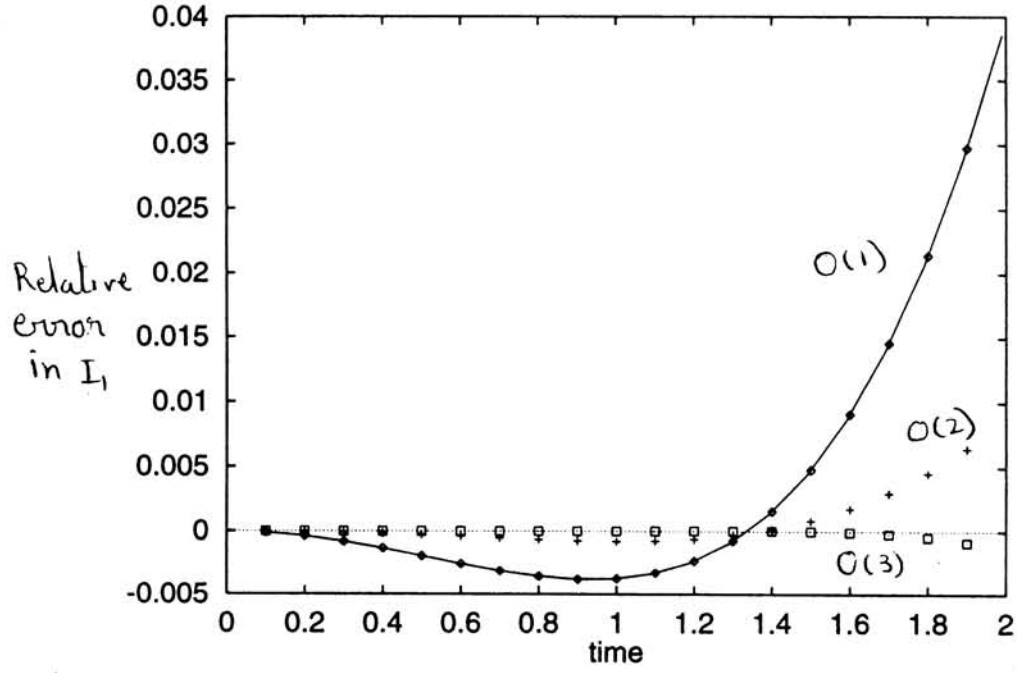

Graph 5.4a: *Relative error in predicted solution for the regular orbit shown in graph 5.1a. $O(1)$, $O(2)$ and $O(3)$ show first, second and third order calculations respectively. The dotted curves are numerical predictions and the solid curve is the analytical prediction.*

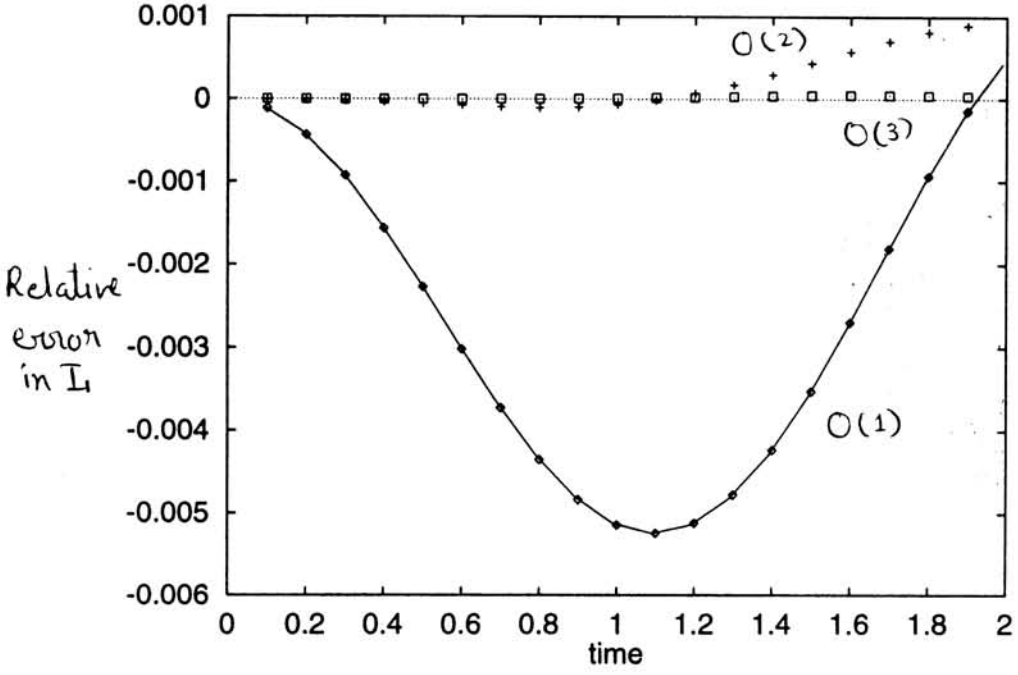

Graph 5.4b: *Same as graph 5.3a, for the regular orbit of graph 5.1b.*

Appendix B: The Generating Functions

$$
\begin{aligned}
F_1 &= \frac{I_2 \sin(\theta_1)}{I_1} + \frac{I_1 \sin(\theta_2)}{I_2} \\
&- \frac{I_2 \sin(\theta_1 - I_1 t)}{I_1} - \frac{I_1 \sin(\theta_2 - I_2 t)}{I_2}
\end{aligned}
$$

$$
\begin{aligned}
F_2 &= \frac{{I_1}^2 t}{4 {I_2}^2} + \frac{{I_2}^2 t}{4 {I_1}^2} \\
&+ \frac{{I_2}^2 t \cos(I_1 t)}{4 {I_1}^2} + \frac{{I_1}^2 t \cos(I_2 t)}{4 {I_2}^2} \\
&+ \frac{{I_2}^2 t \cos(2\theta_1 - I_1 t)}{4 {I_1}^2} + \frac{{I_1}^2 t \cos(2\theta_2 - I_2 t)}{4 {I_2}^2} - \frac{{I_2}^2 \sin(2\theta_1)}{8 {I_1}^3} \\
&+ \frac{\sin(\theta_1 - \theta_2)}{-2 I_1 + 2 I_2} + \frac{I_2 \sin(\theta_1 - \theta_2)}{-4 {I_1}^2 + 4 I_1 I_2} \\
&+ \frac{I_1 \sin(\theta_1 - \theta_2)}{-4 I_1 I_2 + 4 {I_2}^2} - \frac{{I_1}^2 \sin(2\theta_2)}{8 {I_2}^3} \\
&+ \frac{\sin(\theta_1 + \theta_2)}{2 I_1 + 2 I_2} - \frac{I_2 \sin(\theta_1 + \theta_2)}{4 {I_1}^2 + 4 I_1 I_2} \\
&- \frac{I_1 \sin(\theta_1 + \theta_2)}{4 I_1 I_2 + 4 {I_2}^2} - \frac{{I_2}^2 \sin(I_1 t)}{2 {I_1}^3} \\
&- \frac{{I_1}^2 \sin(I_2 t)}{2 {I_2}^3} + \frac{{I_2}^2 \sin(2\theta_1 - 2 I_1 t)}{8 {I_1}^3} - \frac{\sin(\theta_1 - \theta_2 - I_1 t)}{4 I_1} \\
&- \frac{\sin(\theta_1 - \theta_2 - I_1 t)}{4 I_2} + \frac{\sin(\theta_1 + \theta_2 - I_1 t)}{4 I_1} \\
&- \frac{\sin(\theta_1 + \theta_2 - I_1 t)}{4 I_2} + \frac{{I_1}^2 \sin(2\theta_2 - 2 I_2 t)}{8 {I_2}^3} - \frac{\sin(\theta_1 + \theta_2 - I_2 t)}{4 I_1} \\
&+ \frac{\sin(\theta_1 + \theta_2 - I_2 t)}{4 I_2} - \frac{\sin(\theta_1 + \theta_2 - I_1 t - I_2 t)}{2 I_1 + 2 I_2} \\
&+ \frac{I_2 \sin(\theta_1 + \theta_2 - I_1 t - I_2 t)}{4 {I_1}^2 + 4 I_1 I_2} + \frac{I_1 \sin(\theta_1 + \theta_2 - I_1 t - I_2 t)}{4 I_1 I_2 + 4 {I_2}^2} \\
&+ \frac{\sin(\theta_1 - \theta_2 + I_2 t)}{4 I_1} + \frac{\sin(\theta_1 - \theta_2 + I_2 t)}{4 I_2} \\
&- \frac{I_1 \sin(\theta_1 - \theta_2 - I_1 t + I_2 t)}{-4 I_1 I_2 + 4 {I_2}^2}
\end{aligned}
$$

$$\lim_{I_1 \to 0} F_1 = I_2\, t\, \cos(\theta_1)$$
$$\lim_{I_2 \to 0} F_1 = I_1\, t\, \cos(\theta_2)$$

$$\lim_{I_1 \to 0} F_2 = \frac{\sin(\theta_1)}{12\, I_2} \times$$
$$\left(12\, \cos(\theta_2) - 12\, \cos(\theta_2 - I_2\, t) - {I_2}^3\, t^3\, \sin(\theta_1) + 6\, I_2\, t\, \sin(\theta_2) + 6\, I_2\, t\, \sin(\theta_2 - I_2\, t)\right)$$

$$\lim_{I_2 \to 0} F_2 = \frac{\sin(\theta_2)}{12\, I_1} \times$$
$$\left(12\, \cos(\theta_1) - 12\, \cos(\theta_1 - I_1\, t) + 6\, I_1\, t\, \sin(\theta_1) - {I_1}^3\, t^3\, \sin(\theta_2) + 6\, I_1\, t\, \sin(\theta_1 - I_1\, t)\right)$$

Chapter 6

Summary and Conclusions

The TCPT was studied analytically as well as numerically to understand the small denominator problem. We have shown that some of the singularities of the usual perturbation theory can be removed by using TCPT. In the following we summarize the work done.

6.1 Summary

We show that in contrast to CPT, the TCPT predicts generating functions which are finite at all orders. Convergence of the total perturbation series depends on the position of ϵ singularities of $\mathcal{F}$. Though is not possible to study analytical properties of the total TCPT generator $\mathcal{F}$ in general, we show that for two special class of problems analytical properties of $\mathcal{F}$ can be predicted. One of the above mentioned class is of the cases where $\mathcal{F}_{KAM}$ exists. The other class is where the unperturbed Hamiltonian H_0 and the perturbation H_1, both are homogeneous polynomials of different degrees in phase-space variables. For this class we show that the complex time behavior of solutions of the fully perturbed ($\epsilon = 1$) Hamiltonian is related to the complex-ϵ behavior of the canonical transformation equations. Our result suggest existence of natural boundary in complex-ϵ plane (fixed real time) in the canonical transformation equations for this class of Hamiltonian systems. We have also shown that in certain integrable cases where CPT is singular, the TCPT generator can be

calculated exactly and gives convergent results.

Our numerical studies on the H-H system as well as on the KAM-type system shows that the TCPT gives convergent results for small perturbation and small times, with increase in perturbation the radius of convergence decreases. The TCPT gives convergent results for both regular as well as chaotic orbits. Numerical calculation of mapping shows that eventhough there is explicit time-dependence in the generating functions, with increase in order of calculations the results become better. It should be noted that we were able to connect the singularities of the perturbed solutions with singularities in canonical transformations by selecting $\mathcal{F}$ to be identity at $t = 0$ (equivalently $F_{i0} = 0$). If a non-trivial canonical transformation selected at $t = 0$ then it is not possible to predict singularities of the canonical transformation numerically. The mapping results indicate that the radius of convergence of the perturbation theory is defined by the nearest singularity in complex-ϵ plane. The constants of motion calculations show increase in error with increase in energy, we explain this by showing that the singularities at fixed $\mid \epsilon \mid$ appear at smaller real times with increase in energy and thus convergence of the perturbation theory worsen at higher energy values. We also show that chaos only is not responsible for decrease in radius of convergence by applying the TCPT to the anti-H-H system which is integrable. The anti-H-H results also show increase in error in predictions with increase in energy. We explain this result as follows, with increase in energy of the anti-H-H system the motion approaches to the region of phase-space where motion is non-compact which gives rise to decrease in radius of convergence of the perturbation series.

Application of TCPT to the KAM-type system shows similar results as for the H-H system. We show for this case also that TCPT is applicable to both chaotic and regular orbits and gives good agreement with numerical predictions at small time and small perturbations. From the analytical result, we predict that the canonical transformation that transforms the unperturbed Hamiltonian to the perturbed Hamiltonian will have a natural boundary structure in complex-ϵ plane for fixed real real time for both the H-H system and the KAM-type system. In the following section we give conclusions and mention some open questions.

6.2 Conclusions

We have shown that TCPT is more general in the following sense; One can use KAM approximation only in the case of irrational tori and when unperturbed frequencies are non-degenerate. The Gustavson's normal form method can be applied only when the unperturbed frequencies are constant. The TCPT can be used irrespective of the unperturbed frequencies being rational or irrational. Further it is well-known that KAM predicts total breakdown of perturbation theory even under a very small perturbation because it considers generic perturbations whereas TCPT predicts breakdown of perturbation theory from the complex-ϵ singularity structure of the generating function. We suggest that the results of the KAM theory and Gustavson's normal-form method can be better understood with the insight provided by understanding of analytic structure of TCPT generating function.

Existence of singularity in complex-ϵ for fixed real time in the total canonical transformation puts limitation on convergence of the perturbation series. We have shown that if the complex-ϵ singularities of the canonical transformation are isolated the canonical transformation can be analytically continued. Our result shows existence of natural boundary in complex- ϵ plane of the canonical transformation equations for a class of Hamiltonian systems. We suggest that this type of behavior should be investigated for other type of Hamiltonian systems as well, we also suggest that this type of breakdown of the analytical continuation of TCPT generating function can be used to understand breakdown of the KAM tori.

The numerical study of TCPT on the H-H system and the KAM-type system shows that TCPT is applicable to both KAM-type and non-KAM-type systems. The study of anti-H-H system shows that apart from chaos, noncompactness of the potential can also affect convergence properties of TCPT.

One problem in constructing a canonical transformation which transforms an integrable Hamiltonian to a non-integrable one arises due to Lyapunov exponents. Lyapunov exponents measure the exponential rate with which two nearby orbits diverge away from each-other. For a dynamical system with compact dynamics, non-zero Lyapunov exponents indicate chaos. Lyapunov exponents for a system

with continuous dynamics are defined as follows,

$$\lambda = \lim_{t\to\infty} \lim_{d(0)\to 0} \frac{1}{t} \ln \frac{d(t)}{d(0)} \tag{6.1}$$

Where $d(t) = \sqrt{\sum_{i=1}^{n} \delta x_i^2(t)}$ and x_i are dependent variables of the system of differential equations. δx_i is infinitesimal variation along an orbit.

In general Lyapunov exponents do not change under canonical transformations because the equations determining δx_i evolution come from the second order terms of the action principle. At the same time if a canonical transformation exists which transforms an integrable Hamiltonian to a non-integrable Hamiltonian, it should be such that the zero Lyapunov exponents goes to non-zero Lyapunov exponents. We try to understand this situation in TCPT as follows. Calculation of Lyapunov exponents requires calculation of the solutions of EOM for asymptotic time limit. The transformation generated using TCPT can not be calculated for asymptotic time limits in general. The finite order transformation will have algebraic explicit dependence on time in general and so it will be singular in the limit $t \to \infty$. The cases where TCPT generating function can be calculated exactly for all time are all integrable cases. Further our analysis shows that a TCPT transformation that transforms an integrable Hamiltonian to a non-integrable Hamiltonian will have natural-boundary singularity structure in complex-epsilon real time space. In these cases one has to analytically continue the generating function to get a convergent canonical transformation for larger times. If the natural boundary structure is such that the singularities come arbitrarily close to the real time axes then it would not be possible to calculate an exact canonical transformation for larger time. Thus we are not able to come to a definite conclusion about conservation of the Lyapunov exponents under a TCPT transformation.

Bibliography

[1] Poincare in *New methods of celestial mechanics* vol. I, II and III, translated by D. L. Goroff (American Institute of Physics, 1993)

[2] Giacaglia in *Perturbation methods in non-linear systems* (Springer-Verlag, 1972)

[3] Berry M.V. in, *Topics In Nonlinear Dynamics A Tribute to Sir Edward Bullard*, edited by S.Jorna (American Institute of Physics, New York, 1978) p. 16-120.

[4] Arnold V.I., *A theorem of Liouville concerning integrable problems of dynamics*, Sibirsk. mat. zh. 4, p. 417-474 (1963)

[5] Ziglin S.L., *Branching of solutions and non-existence of first integrals in Hamiltonian mechanics*, Functional Anal. Appl. 16, p. 181-189 (1983); 17, p. 6-17 (1983)

[6] Yoshida H. *Existence of exponentially unstable periodic solutions and the non-integrability of homogeneous Hamiltonian systems*, Physica 21 D, p. 163-170 (1986) and *A criterion for the non-existence of an additional integral in Hamiltonian systems with a homogeneous potential*, Physica 29 D, p. 128-142 (1987)

[7] Ramani A., Grammaticos B. and Bountis T.C., *The Painleve property and singularity analysis of integrable and non-integrable systems*, Physics Reports, 180, p. 159-245 (1989)

[8] Goldhirsch I., Sulem P. and Orszag S.A., *stability and Lyapunov stability of dynamical systems*, Physica 27 D, p. 311-337 (1987)

[9] Henon M., *On the numerical computation of Poincare maps*, Physica 5 D, p. 412-414 (1982), also see [15] and [22].

[10] Nayfeh A.H., *Introduction to perturbation techniques*, (John Wiley and sons, 1981)

[11] Arnold V.I., *Mathematical methods of classical mechanics*, second edition (Springer-Verlag, 1988)

[12] Wiggins S., *Global bifurcations and chaos*, Applied Mathematical Sciences, vol. 73, (Springer-Verlag, 1988)

[13] Escande D.F., *Stochasticity in classical Hamiltonian systems; universal aspects*, Physics Reports, 121, p. 165-261 (1985)

[14] Guckenheimer J. and Holmes P., *Non-linear oscillations, dynamical systems and bifurcations of vector fields*, Appl. Math. sci., vol. 42, (Springer-Verlag, Berlin, 1983) and Arnold V.I. in *Geomerical methods in the theory of ordinary differential equations*

[15] Gustavson F.G., *On constructing formal integrals of a Hamiltonian system near an equilibrium point*, Astron. J., 71, p. 670 (1966)

[16] Goldstain H., *Classical mechanics*, second edition, (Narosa publishing house, 1992)

[17] Sudarshan E.C.G. and Mukunda N., *Classical dynamics: A modern perspective*, (John Wiley and sons, 1974)

[18] Deprit A., *Canonical transformations depending on a small parameter*, Cel. Mech., 1, p. 12-30 (1969) and references therein.

[19] Kaufman A.N., *Topics In Nonlinear Dynamics A Tribute to Sir Edward Bullard*, edited by S.Jorna (American Institute of Physics, New York, 1978) p. 286

[20] Sitaram B.R. and Mitaxi P. Mehta, in *Time Dependent Canonical Perturbation Theory:I:General Theory*, Pramana-J. Phys., 45, p. 141-148 (1995)

[21] Chang Y. F., Tabor M. and Weiss J., *Analytic structure of the Henon-Heiles Hamiltonian in integrable and non-integrable regimes*, J.Math.Phys. 23, p. 531 (1982) **23**, 531(1982) also see Chang Y.F., Greene G.M., Tabor M. and Weiss J., *The analytic structure of dynamical systems and self-similar natural boundaries.*, Physica 8 D, p. 183-207 (1983)

[22] Henon M. and Heiles C., Astron. J. 69, p. 73 (1964)

[23] Contopoulos G. and Polymilis C., *Approximations of the 3-partcle Toda lattice*, Physica 24 D, p. 328-342 (1987)

[24] Mehta M.P. and Sitaram B.R., *Time Dependent Canonical Perturbation Theory:II: Application to the Henon-Heiles system*, Pramana-J. Phys., 45, p. 149-164 (1995)

[25] Chang Y.F. and Corliss G., *Ratio like and recurrence relation tests for convergence of series*, J. Inst. Maths. Applics., 25, p. 349-359 (1080)

[26] Lyness J.N. and Sande G. *ENTCAF and ENTCRE: evaluation of normalized Taylor coefficients of an analytic function.* Comm. of the ACM, 14, p. 669-675 (1971)